REVIEW

Go beyond the limit: Rationally designed mixed-dimensional perovskite/semiconductor heterostructures and their applications

Weili Yu,[1,*] Feng Li,[2,*] Tao Huang,[1] Wei Li,[1] and Tom Wu[3,*]

*Correspondence: weili.yu@ciomp.ac.cn (W.Y.); feng.li2@sydney.edu.au (F.L.); tom.wu@unsw.edu.au (T.W.)

Received: May 27, 2022; Accepted: December 18, 2022; Published Online: December 20, 2022; https://doi.org/10.1016/j.xinn.2022.100363

GRAPHICAL ABSTRACT

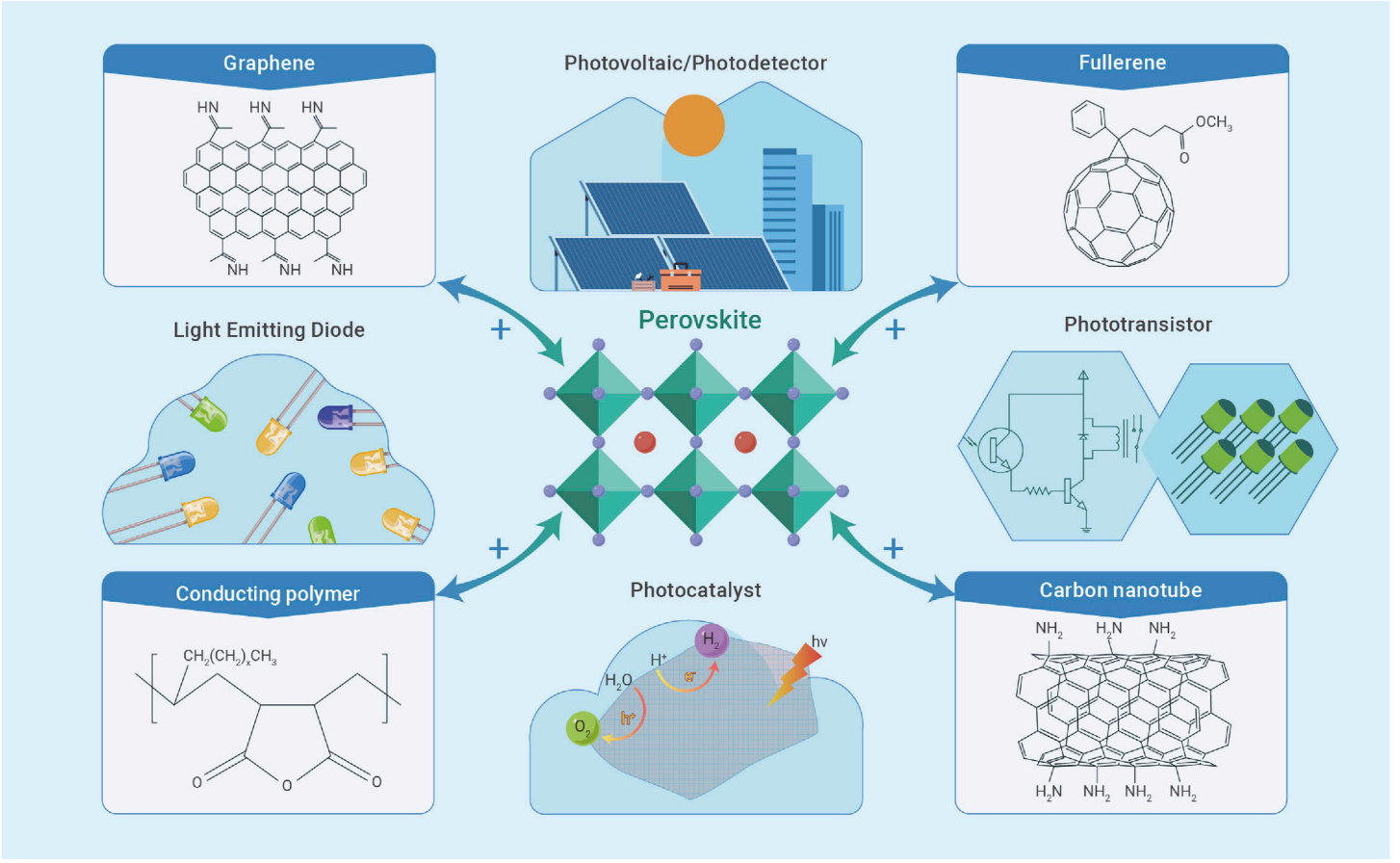

PUBLIC SUMMARY

- Heterojunctions endow perovskites with diverse structures and desirable properties.
- Heterojunctions bestow novel phenomena and exotic physical effects on perovskites.
- Optoelectronic device performance can be greatly enhanced by heterojunctions.

REVIEW

Go beyond the limit: Rationally designed mixed-dimensional perovskite/semiconductor heterostructures and their applications

Weili Yu,[1,*] Feng Li,[2,*] Tao Huang,[1] Wei Li,[1] and Tom Wu[3,*]

[1]GPL Photonics Laboratory, State Key Laboratory of Luminescence and Applications, Changchun Institute of Optics, Fine Mechanics and Physics, Chinese Academy of Sciences, Changchun 130033, China

[2]School of Physics, The University of Sydney, Sydney, NSW 2006, Australia

[3]School of Materials Science and Engineering, University of New South Wales, Sydney, NSW 2052, Australia

*Correspondence: weili.yu@ciomp.ac.cn (W.Y.); feng.li2@sydney.edu.au (F.L.); tom.wu@unsw.edu.au (T.W.)

Received: May 27, 2022; Accepted: December 18, 2022; Published Online: December 20, 2022; https://doi.org/10.1016/j.xinn.2022.100363

Citation: Yu W., Li F., Huang T., et al., (2023). Go beyond the limit: Rationally designed mixed-dimensional perovskite/semiconductor heterostructures and their applications. The Innovation **4(1)**, 100363.

Halide perovskite heterojunctions rationally integrate the chemical and physical properties of multi-dimensional perovskites and judiciously chosen semiconductor materials, offering the promise of going beyond the limit of a single component. This emerging platform of materials innovation offers fresh opportunities to tune material properties, discover interesting phenomena, and enable novel applications. In this review, we first discuss the fundamentals of forming heterojunctions with perovskites and a wide range of semiconductors, and then give an overview of the research progress of halide perovskite heterojunctions in terms of their optical, electrical, and mechanical properties, focusing on how the heterojunction tunes the energy band structure, electrical transport, and charge recombination behaviors. We further outline the progress of perovskite-based heterojunctions in optoelectronics. Finally, the challenges and future research directions for perovskite/semiconductor heterojunctions are discussed.

INTRODUCTION

In the past decade or so, the extraordinary optoelectronic properties of metal halide perovskite materials have aroused widespread interest and intensive research by scientists from all over the world majoring in material science, chemistry, physics, electronics, and even biology. Research on metal halide perovskite has yielded a series of exciting results in solar cells (or photovoltaics), light-emitting diodes (LEDs), lasers, field-effect transistors (FETs), and other fields, pushing forward both fundamental and applied research. In the photovoltaic field, the solar-to-electricity conversion efficiency of 25.6% has been achieved for single-junction perovskite,[1] as well as efficiency of around 30% for the tandem perovskite solar cells.[2] In the field of LEDs, the high external quantum efficiency (EQE) values of 12.3% and 22% have been achieved in the blue and green devices, respectively.[3] In the field of electronics, the carrier mobility of over 50 cm^2/Vs has been demonstrated for p-channel perovskite thin-film transistors.[4] Despite the great progress that has been made, the fundamental properties responsible for the high performance of halide perovskite devices have yet to be fully elucidated, and there remains lots of room for further advancing the perovskite technologies.[5]

To overcome the inherent limitations of perovskites, several approaches have been explored to regulate the composition, structure, and properties. Currently, the widely used methods include doping, surface passivation, and combining with other functional materials. The doping strategy aims to tune the properties of perovskite by introducing different atoms at specific lattice positions. The doping strategies can be categorized into intrinsic doping and extrinsic doping strategies, which depend on the characteristics of charged defects in the lattice structure.[6] The former is achieved by changing the constituent chemical potentials or the precursor ratio during synthesis; the latter introduces impurity atoms into the lattice structure. Elements such as Bi, La, and Mn have been introduced into perovskites as extrinsic dopants with modified properties.[7–11] More information on the doping strategy is available elsewhere.[12,13] For the surface passivation strategy, recent works showed that the molecular passivation agents at the perovskite surface or grain boundary inhibit trap-mediated non-radiative charge recombination, resulting in improved solar cell efficiency and stability.[14–16] Some molecular agents such as theophylline, caffeine, and theobromine have been systematically investigated for defect passivation; when N–H and C=O are in an optimal configuration in the molecules, the formation of hydrogen bond between N–H and I would assist the primary C=O binding with the antisite Pb defects and maximize the passivation effect.[16,17] The passivation strategies are continually advancing to improve the device performance.[18–23]

To further expand the material properties, improve device performances, and enhance the compatibility of perovskites with existing protocols, more challenges must be confronted. For example, the absorption spectra of perovskites are still confined to the visible range; the carrier transport and separation properties of halide perovskite are still less efficient than its counterparts (e.g., doped silicon). A strategy for breaking through these limitations has emerged; i.e., constructing the homo- or mixed-dimensional perovskite/semiconductor heterojunctions by introducing other semiconducting components into perovskites. The macro- or micro-scaled heterojunctions formed at the interface between perovskites and other semiconductors may bring more possibilities for designing and modifying the properties of perovskite-based systems, thus allowing for more promising applications.[12]

In this review, we present the recent research progress on halide perovskite-based heterostructures and composites, with an emphasis on the mechanisms of optimizing the physical properties and improving the device performance. We first briefly discuss the fundamentals of metal halide perovskites and the related heterojunctions, and then highlight how the heterojunctions affect and regulate the optical, electrical, and mechanical properties, as well as the stability of metal halide perovskite-based heterostructures, focusing on the underlying physical mechanism. Furthermore, the applications of perovskite-based heterojunctions in promising fields including solar cells, LEDs, photodetectors/transistors, and photocatalysts are reviewed. Finally, the possible challenges and outlook for future development of perovskite-based heterojunctions are discussed.

PEROVSKITE-BASED HETEROJUNCTIONS

Perovskites with dimensional diversity

The three-dimensional (3D) perovskites have a common structure with a general chemical formula of ABX_3 ($A = Cs^+$, $CH_3NH_3^+$ (MA^+), or $[HC(NH_2)_2]^+$; $B = Pb^{2+}$, Ge^{2+}, or Sn^{2+}; $X = Cl^-$, Br^-, or I^-). As shown in Figure 1A, there are two ways to classify the perovskites in terms of reduction of dimensionality. The first one is based on the morphology of halide perovskites; that is, as the perovskite crystal size decreases continuously, the perovskites change from 3D bulk to two-dimensional (2D) plate, then one-dimensional (1D) wire and zero-dimensional (0D) quantum dots (QDs).[13,24–27] The second one is based on lattice structure dimensions and phase space features. When the A site is occupied by large organic groups, the low-dimensional halide perovskites can be obtained. Specifically, the quasi-2D halide perovskites share the formula of $(A')_m(A)_{n-1}B_nX_{3n+1}$, where A′ is a large organic group, and either monovalent (m = 2) or divalent (m = 1) cations can intercalate between the anions of the 2D perovskite sheets. Depending on the organic layer composition and phase space, three types of 2D perovskite can be achieved; i.e., Ruddlesden-Popper, alternating cation (ACI), and Dion Jacobson (DJ) crystal phases. Furthermore, metal halides with 1D and 0D molecular structures can also form, offering versatile composition engineering opportunities.[26,27]

The change in morphology and lattice structure of halide perovskites can lead to dramatic variations in their optical and electrical properties; e.g., the quantum confinement, dielectric effect, or anisotropic transport.[30] As shown in Figure 1B, the band alignments and bandgaps of halide perovskites vary with different compositions, which offer rich opportunities to form heterojunctions within

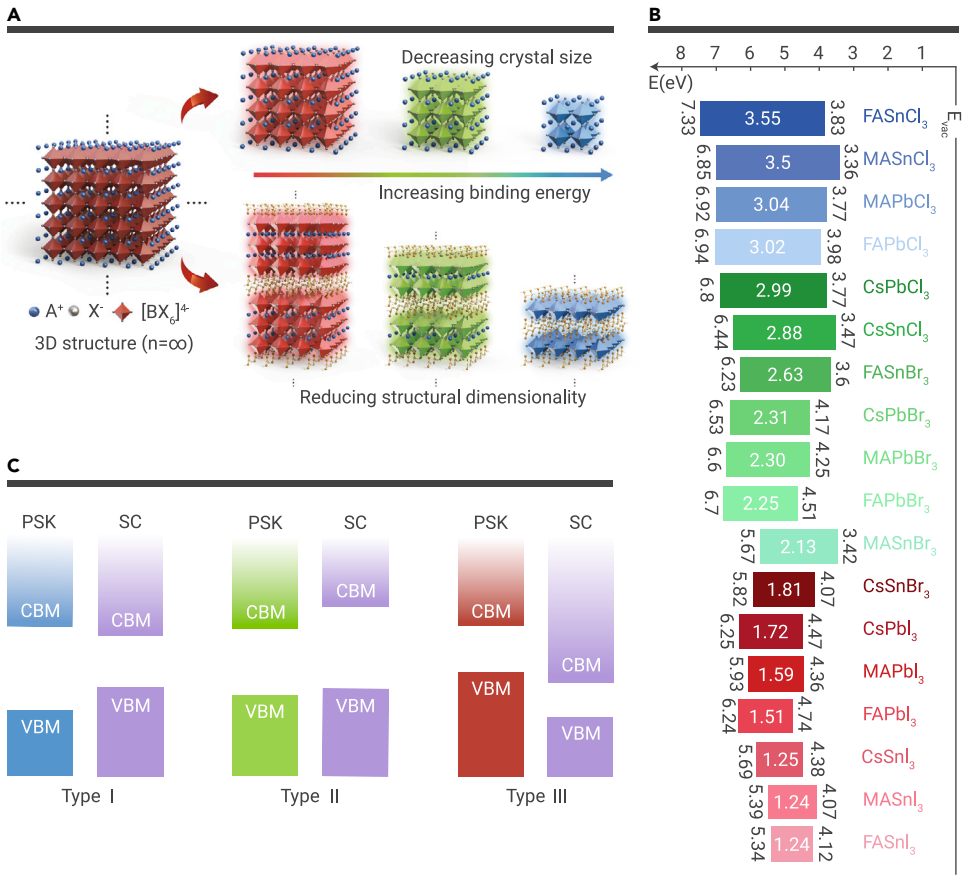

Figure 1. Fundamentals of perovskites and heterojunctions (A) Schematic illustration of perovskite with decreased size and reduced dimension.[28] Copyright 2021, Springer Nature. (B) Schematic energy-level diagram of the representative metal halide perovskites.[29] Copyright 2019, Springer Nature. (C) Three types of heterojunctions between perovskite and semiconductor. PSK, perovskite; SC, semiconductor, VBM, valence band maximum; CBM, conduction band minimum.

themselves and with other functional materials. Based on the high diversity of sizes, structures, and chemical compositions, the inherent properties of the halide perovskites show significant tunability.

Formation of perovskite heterojunctions

The heterostructures based on functional semiconductors define the essential building blocks for modern electronics and optoelectronics, including solar cells, FETs, LEDs, and various sensing devices. Generally, the heterojunction refers to the interfacial region between the two contacted functional semiconductors, and it can be beneficial for improving the carrier separation and transport performance by forming built-in electric fields within the formed heterojunctions. Figure 1C displays the band alignments of three typical heterojunctions. According to the energy band alignments of the involved semiconductors, three types of semiconductor-based heterojunctions can be formed. As for the type I heterojunction, the bottom of the conduction band (CB) and the top of the valence band (VB) of semiconductor A are higher and lower, respectively, than those of the semiconductor B with the narrow bandgap. In the type II heterojunctions, both the CB and VB energy levels of semiconductor A are higher than that of semiconductor B, respectively, which means that the bandgap of the two semiconductor materials is partially overlapped but not embedded. The type III heterojunction is a little bit similar to the type II heterojunction, except that the staggered bandgaps between the two semiconductor materials do not overlap.[31] For the type I heterojunctions, both the holes and electrons generated in the semiconductor A will move to the semiconductor B and then could recombine within the semiconductor B or at the interface, thereby effectively enhancing the luminescence properties and performance. Thus, type I heterojunctions are useful for applications in LEDs and lasers, etc. For the type II heterojunctions, hole/electron pairs generated within the semiconductor will efficiently separate at the interface and move in opposite directions, facilitating the charge carrier transfer and leading to the enhancement of electrical current. Type II heterojunctions are widely employed for high-performance solar cells and photodetectors (PDs) since the photo-induced electrons and holes can be well spatially separated with long-lived interlayer excitons. Type-III heterojunctions are often exploited for designing tunneling devices.

The variable composition and mixed ionic-electronic transport properties of halide perovskites provide more possibilities for designing novel heterojunctions. Due to the electronic/ion coexistence nature of halide perovskites, the interaction forces between perovskites and semiconductors include covalent bonds, ionic bonds, hydrogen bonds, and van der Waals forces. These interaction forces can be selectively utilized to design heterojunctions with desired interface properties. As shown in Figure 2A, the cations and anions on the surface of the perovskite QDs (PQDs) may form ionic bonds as ion pairs; the ammonium cations replace the surface A-cations, while halides or carboxylates attach to the surface and remain charge neutral may form covalent bonds. The perovskite and 2D materials may interact with van der Waals forces in stacked heterostructures. Taking PQDs as an example, the covalent bonds between PQDs and ligands can be classified into three types; i.e., L type (two-electron-donor ligand, as Lewis base), Z type (two-electron acceptor ligand, as Lewis acid), and X type (single-electron acceptor ligand, as Lewis acid).[32,33] The ligands can be utilized to achieve following functions: to improve the luminescent properties, enhance the electronic coupling, or increase stability.[34–36] For example, phenylalkylammonium passivated perovskites show greatly improved luminescent property.[37] 3-Aminopropanioc acid-coated ZnO can help form highly crystalline hybrid perovskite $MAPbI_3$ films with improved electronic coupling and reduced pinholes.[38] Some other ligands, such as trioctylphosphine oxide, can greatly improve the stability of PQDs.[39] In addition to PQDs, the above ligands can also be selectively used to modify other perovskite materials, such as films and bulks.

Figure 2B summarizes the typical functional semiconductors that can form heterostructures or heterojunctions with halide perovskites, which include organic polymers (or big molecules), small molecules, 2D materials, 1D materials such as carbon nanotubes (CNTs), nanocrystals (NCs), and inorganic semiconductors such as silicon wafers.[32] Unlike the doping strategies that directly change the energy band structure and electronic properties, the introduction of additional semiconductor components will form heterojunctions with halide perovskites, leveraging the complementary properties of the constituents and modifying the charge carrier concentration, distribution, and transport properties. To this end, the optical, electrical, and mechanical properties of the perovskite-based heterostructures and composites would be in turn affected and tuned, aiming at obtaining the desirable material properties. Considering the possible differences between halide perovskites and other semiconductor materials, some specific issues need to be considered; i.e., the lattice of colloidal QDs (CQDs) may not match the perovskite crystal structures well in most cases, the interfacial chemical treatment processes and structural designing are highly rewarding.

For halide perovskites containing an organic component with amino groups, the surface of the introduced semiconductor material must be properly treated to promote the contact and heterogeneity. Amination or carboxylation of the introduced functional semiconductors via interfacial engineering method is often utilized. The semiconductor materials typically employ the cations and/or anions as the ion pairs to bind onto the surface of perovskite, where the ammonium cations would replace the surface A-cations of halide perovskites, and the halides or carboxylates would attach to the surface and retain the charge. Figure 3 shows

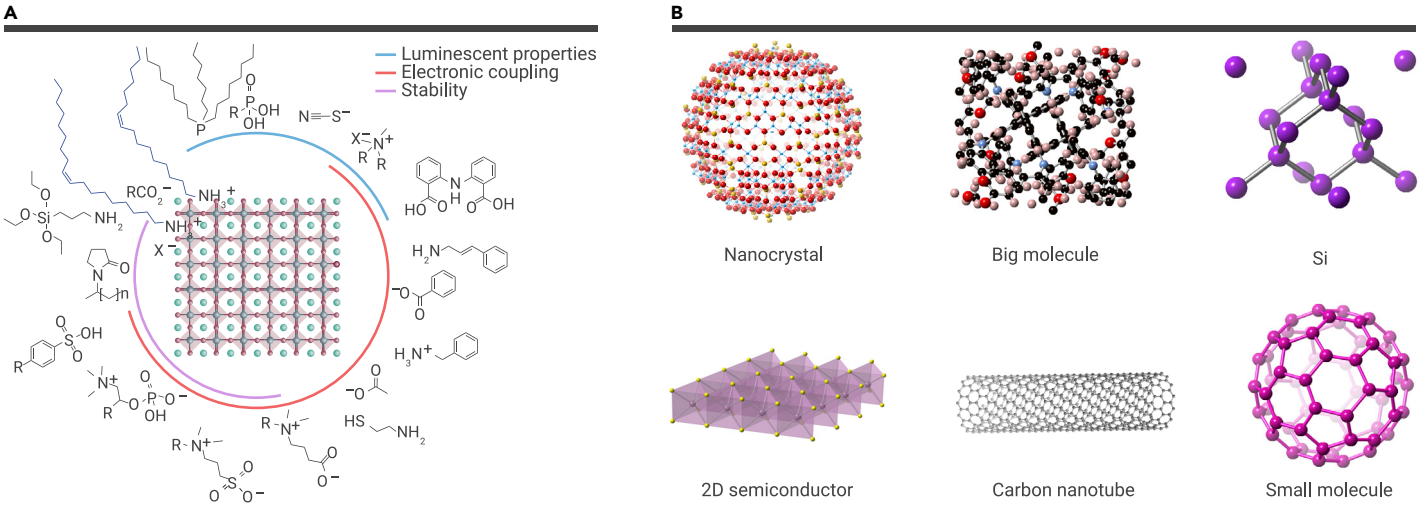

Figure 2. Ligands between halide perovskite and different semiconductors (A) Various ligands that have been adopted in the synthesis of perovskite nanoparticles.[32] Copyright 2020, Springer Nature. (B) Illustration of some typical semiconductors that can form heterojunctions with perovskites, including NCs, big molecules (or polymers), Si, 2D semiconductors, carbon nanotubes, and small molecules.

the typical strategies for the interfacial treatments of homo- or mixed-dimensional heterojunctions by combining perovskite with other functional materials. As schematically shown in Figure 3A, the PbS QDs were stabilized using methylammonium iodide (MAI) to realize atomic-level coherence between PbS and $MAPbI_3$, and the PbS QD lattice embedded in the 3D perovskite $MAPbI_3$ matrix matches well with the perovskite structure. In the inorganic halide perovskite/perovskite heterostructures, such as colloidal $CsPbX_3$—$Pb_4S_3Br_2$ (X = Cl, Br, or I), the shared plane of lead atoms at the interface, which is almost unaltered within both the chalcohalide and the perovskite structures, was demonstrated to play an important role for the well-defined epitaxial heterostructures (Figure 3B).[40] These works underscore the feasibility of designing high-quality heterostructures with halide perovskite and inorganic materials with a sharp and atomically resolved epitaxial interface.

Various organic semiconductors (including polymers or small molecules) have been used to make the heterostructures with halide perovskites for various optoelectronic devices. The introduced organic materials can act as either the charge transport layer or the active layer. The organic semiconductor(s) could affect the device performance and/or stability via different mechanisms, such as extracting charge carriers, tuning the orientation of perovskite crystals, and passivating the perovskite film surface. As shown in Figure 3C, the grazing incident wide-angle X-ray scattering (GIWAXS) measurement results indicate that the existence of a low-cost and stable conjugated polymer poly[(thiophene)-alt-(6,7-difluoro-2-(2-hexyldecyloxy)-quinoxaline)] (PTQ10) layer can effectively reduce the tendency for perovskite decomposition and maintain the high crystallinity of perovskite film, resulting in a champion power conversion efficiency of 21.2% with a great ambient and thermal stability.[41]

Low-dimensional semiconductors, due to their excellent electrical and optical features and promising mechanical behaviors, have been widely employed to make the halide perovskite-related heterostructures and composites, aiming at high-performance electronic or opto-/electronic devices. Except for experimental works, there are also some related theoretical investigations on the interfacial structure and properties. Taking the CNTs as an example, Tan et al. systematically performed the density function theory (DFT) calculations to check the interfacial electronic structure and optical absorption of the $MAPbI_3$/CNTs heterojunction systems.[42] As shown in Figure 3D, the formed heterostructures display the different charge carrier transfer processes and termination dependence of band alignment; i.e., the CNTs/PbI_2-terminated $MAPbI_3$ (001) surface heterojunction has a type I band alignment, while the CNTs/MAI-terminated $MAPbI_3$ (001) surface forms a type II band alignment. In addition, Kim et al. experimentally and theoretically demonstrated the specific interfacial interaction between organic-inorganic hybrid perovskites and nitrogen-doped CNTs, which include the following processes: (1) negatively charged pyridinic N-dopant site generates initial interaction for nucleation, (2) perovskite structure is predominantly formed at N-dopant site when interacting with MA^+ ion rather than Pb^{2+} ion, and (3) the $-NH_3^+$ group of MA^+ ion is modified into a $-NH_2$-like form by sharing a proton with lone-pair electrons of pyridinic N-dopant site. The transmission electron microscopy (TEM) measurements showed that the N-dopant CNTs could be uniformly wrapped by halide perovskite crystals (Figure 3E), which indicated that N-dopant sites within CNTs were primarily responsible for the well-defined heterostructures.[43] Such a strategy could be used to treat the surface of carbon-based low-dimensional materials (including graphene, fullerenes, or CNTs) for forming the perovskite-based heterojunctions.

Table 1 summarizes the types, advantages, and applications of various perovskite/semiconductor heterojunctions. The introduced functional semiconductors could play different roles in forming the heterojunction(s) with halide perovskites. For example, the functions of organic polymers within the perovskite/polymer composites include optimization of perovskite crystal morphology, promoting heterogeneous nucleation, passivation of surface or grain boundary, improving heat or moisture stability, enhancing the mechanical resilience, self-healing effect, self-aggregation properties, facilizing the reaction between the precursors, such as PbI_2 and MAI, extending the special electrical and optical properties, and improving the transport of charge carriers.

PHOTOPHYSICAL PROPERTIES

The photophysics of halide perovskites depends on their sizes, structures, and compositions, which directly affect their optical, electrical, and photoelectric conversion properties. The perovskites also suffer from moisture-induced photodegradation and thermal and solvent instabilities, which adversely affect their structural integrity, reduce their long-term stability under ambient conditions, and eventually lead to blueshifts and quenches of the photoluminescence (PL) emission.[29,51] In the following content, the beneficial effects of halide perovskite-based heterojunction on their absorption, PL, light dynamics, and nonlinear optical properties will be discussed.

Broadening the absorption range

A common but intrinsic shortcoming of the perovskites in both the bulk and nanoscale forms is that they can only convert the UV-visible light (280–800 nm) or a very narrow range in the standard AM-1.5G sunlight spectrum (280–2,500 nm). The near-infrared (NIR) light, which represents around 52% of the total solar irradiance, may generate a drastic thermal heating effect that shortens the duration of the relevant devices, while the solar energy conversion efficiency may be further increased if the NIR light can be properly utilized. Therefore, it is of pivotal importance to extend the absorption window of halide perovskites into the NIR range, so that the optoelectronic capabilities, in terms of energy conversion, light detection, and signaling, can be extended to the NIR region to satisfy various purposes.[75] In this regard, two strategies are available. One is combining perovskite with narrow-bandgap semiconductors, including CQDs, CNTs, 2D materials, or organic semiconductors. The other one is utilizing

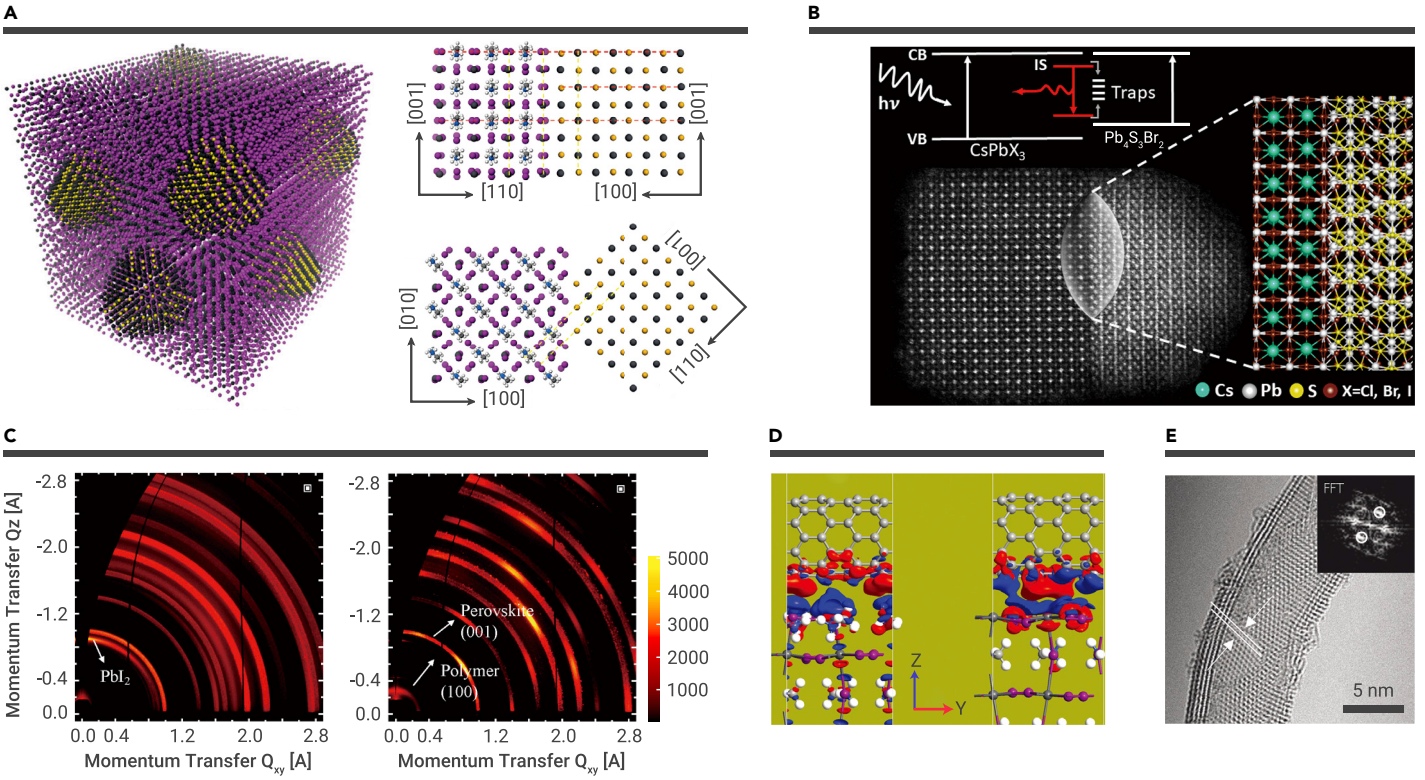

Figure 3. Various heterojunctions between perovskites and different semiconductors (A) Heterogeneous matrix composed of $MAPbI_3$ perovskite and PbS NCs. The modelling of PbS and $MAPbI_3$ crystal structures and their interfaces indicates that perovskite matches well with PbS in both the x-z and the x-y planes.[39] Copyright 2015, Nature Publishing Group. (B) High-resolution scanning tunneling electron microscopy (STEM) image of a single heterostructure composed of all-inorganic perovskite $CsPbBr_3$ and the $Pb_4S_3Br_2$ domains.[40] Copyright 2021, American Chemical Society. (C) GIWAXS analysis and characterization of perovskite films with and without polymer treatments. (Left) GIWAXS 2D patterns of the control $FAPbI_3$ sample and (right) the one treated with PTQ10 during a thermal annealing process.[41] Copyright 2018, American Chemical Society. (D) The calculated 3D charge density differences of two possible stacking cases of the $MAPbI_3$/CNTs heterojunctions. The red and blue regions represent the charge accumulation and the depletion, respectively.[42] Copyright 2021, Royal Society of Chemistry. (E) TEM images of CNTs and $MAPbI_3$/CNTs hybrids. The inset shows the fast Fourier transform (FFT) result.[43] Copyright 2019, Wiley-VCH.

nonlinear optical property to tune the absorption range, which will be discussed in the following section.[75,76]

Narrow-bandgap semiconducting CQDs, such as PbS and PbSe, are widely utilized for light absorption and detection in the NIR regime. By introducing the narrow-bandgap CQDs into the halide perovskite matrix, both absorption and luminescence signatures of the obtained systems will change according to their component ratios. As shown in Figure 4A, the absorbance of the perovskite-based matrix can broaden from the visible into the NIR range.[39,77] Due to their complementary properties, both the halide perovskite and CQDs contributed to light absorption, resulting in the generation of more excitons. The CNTs and $MAPbI_3$ composites can not only combine the high absorption coefficient of both materials for improving the efficiency of light utilization but also enhance absorption by external conditions like the terminations (i.e., surface compositions or groups). DFT calculations showed that the band alignment in the perovskite/CNTs heterojunctions is subject to the terminations of hybrid perovskite materials and the applied electrical potentials.[42] When integrated CNTs with the PbI_2 surfaces of $MAPbI_3$ perovskite, the optical absorption of the resultant heterojunctions could be enhanced in the NIR region, and it is nearly equivalent to the isolated PbI_2-terminated slab in the visible region. The absorption coefficient of the CH_3NH_3I surface in $MAPbI_3$/CNTs is smaller than that of the PbI_2-surface $MAPbI_3$/CNTs heterojunction, which is mainly attributed to the termination dependence of the electronic states of the (001) surface of $MAPbI_3$.[42,78]

Enhancing/quenching photoluminescence

The perovskite/semiconductor heterostructures can be utilized to enhance, quench, or shift the PL of the obtained perovskite composites. By tuning the band alignments of components, both the type I and type II heterojunctions may be achieved, and the pathway for the charge transfer between the individuals is thus highly tunable. When the energy bands of the introduced semiconductor materials, such as CQDs, lie within the bandgap of the halide perovskite materials, the type I heterojunction can be formed. This type of heterojunction can facilitate the separation of the excitons, and the photo-induced carriers can transfer to the small-gap CQDs, leading to the greatly enhanced photoluminescence quantum efficiencies (PLQEs), the redshifted luminescence, and the increased Stokes shift.[39] In the perovskite/semiconductor composites, the charge carriers might generate in either the halide perovskites or the additional semiconductors under light illumination and then transfer to the perovskite/CQDs interfaces. The carrier transfer efficiency from halide perovskite to CQDs can go up to a value exceeding 80% at the highest CQD loading.[39] Unlike the pure perovskites, the charges will recombine at the heterojunction interfaces and grain boundaries, thus affecting the light-emitting properties. As shown in Figure 4B, the PL value of halide perovskite could be highly quenched in the perovskite/PbS heterostructures. The PL intensity and wavelength of heterostructures also show the CQD concentration dependence. When the concentration of CQD increases, PL blueshifts may occur due to the tensile strain caused by lattice mismatch between CQDs and perovskites that slightly expanded the CQD lattice, leading to the increased bandgap of the resultant system. In addition, as the CQD concentration increased, the absorption spectrum redshifts would occur, consistent with the increased inter-dot interaction and the reduced quantum confinement effect, as shown in Figure 4C. This might be attributed to the partial dot fusion at the high concentrations of CQDs, which thus shrank the bandgap of the resultant system.[39] Liu et al. used the strained QDs as the nucleation centers to drive the homogeneous crystallization of the perovskite matrix. The formed type I band alignment ensures that the QDs could work as charge acceptors and radiative emitters. The new matrix materials may suppress Auger bi-exciton recombination and show bright luminescence at high excitation, whereas the control materials exhibit severe bleaching.[80] In this case, rapid charge tunneling through the interfaces within the matrix and the subsequent charge injection into the embedded QDs were confirmed, indicating the ultrafast charge transfer from halide perovskites to smaller bandgap acceptors.[39]

Table 1. The advantages and applications of various heterojunctions formed by halide perovskites and other semiconductors

	Heterojunctions	Advantages of heterojunctions	Applications	References
1	PSK/PSK	broaden absorption improve stability promote separation of photo-generated excitons and carrier diffusion	PV photo memory PC	Imran et al., Lin et al., Zhao et al.[40,44,45]
2	PSK/Si	improve NIR light absorption minimize light reflection at the surface improve long-term stability	PV PD LEDs PT	Xu et al., Al-Ashouri et al., Wei et al., Hou et al., Kim et al.[2,46,47–50]
3	PSK/polymer	enhance electron/hole conductivity promote reaction between PbI_2 and MAI improve stability against moisture introduce novel electrical and optical properties improve heat stability	PV PD PC LED PT	Liang et al., Liu et al., Kim et al., Li et al., Xie et al.[51,52–55]
4	PSK/small molecules	tune the absorption and photoluminescence properties passivate vacancies construct various heterogeneous junction improve exciton generation, charge transport and extractionsuppress charge recombination	PV PD PC LED	Lai et al., Li et al., Sun et al.[56,57,58]
5	PSK/CQDs	tune the absorption and photoluminescence property improve conductivity construct various heterogeneous junctions improve exciton generation, charge transport and extraction suppress charge non-radiative recombination balance hole and electron concentration	PV PD PC PCd LED	Ning et al., Gong et al., Xu et al., García de Arquer et al., Chen et al.[39,59,60,61,62]
6	PSK/2D materials	improve conductivity as electron/hole transport layer as photoactive layers fast electron extraction additive for photoactive layers	PV PD PC LED PT	Chen et al., Ma et al., Zhu et al., Wang et al.[63,64,65,66]
7	PSK/CNT	as flexible electrode enhance light absorption enhance carrier transport facilitate charge extraction suppress charge recombination	PV PD PC LED PT	Bati et al., Avery et al., Luo et al.[67,68,69]
8	PSK/metal oxides	electron/hole transporting layer improve conductivity facilitate charge extraction enhance carrier's separation	PV PD LED PT	Qian et al., Lindbad et al., Gao et al., Zhang et al., Guan et al.[70,71,72–74]

PSK, perovskite; PV, photovoltaic; PD, photodetector; PT, phototransistor; PC, photocatalysis; PCd, photoconductor; LED, light-emitting diode.

Besides CQDs, some other semiconductor materials are also utilized to form perovskite-based heterojunctions.[21,40,81–86] For the perovskite/ polymer heterostructures, the addition of a variety of polymers into the perovskite materials could improve photoluminescence quantum yield (PLQY) values of resultant composites or heterostructures by passivating the surface of perovskite, by forming individually dispersed NC cores within an encapsulating polymer matrix. Such a strategy of forming heterostructures leads to a significant enhancement in PLQY due to the spatial separation of the perovskite NCs and hence the deactivation of energy transfer to dark crystals.[87] Briefly, for the pure halide perovskite films, the grain boundaries exhibit radiative/non-radiative recombination.[88] For the perovskite-based heterojunctions, the recombination may happen at the grain boundaries and perovskite/semiconductor interfaces.[59,89] These additional interfaces may bring more opportunities for developing high-efficiency light-emitting devices.[77]

Tuning the photophysical dynamics

The photophysical dynamics of halide perovskites will be significantly affected once heterojunctions are formed between perovskites and other semiconductor materials. The pathways of charge transfer will change according to the types of the heterojunctions formed, leading to more efficient or blocked charge transfer. Pump-probe technique or time-resolved photoluminescence spectroscopy can offer in-depth information on the charge transfer dynamics. In the type I perovskite heterojunction, for example, the average PL lifetime was significantly shortened from 4.52 ns for the pure $MAPbBr_3$ QDs to 2 ns for the QDs-in-perovskite matrix.[77] With the increase in the mass proportion of QDs, the lifetime of the composited matrix was shortened accordingly. These indicated that, because of the perovskite/QDs heterojunction, the photo-generated carriers could be separated at the interface more efficiently. The resulting PL lifetime attenuation accelerates the photo-induced carrier separation process with the increase of the QDs ratio. The higher ratio of the incorporated QDs can thus result in a smaller average PL lifetime, as shown in Figure 4D. These findings on the carrier transport kinetics show the significance of heterojunction in the charge transfer process, which is beneficial for fabricating high-performance solar cells or photodetectors.[77,90]

Radiative and non-radiative recombination

The type II heterojunction favors the separation of excitons, whereas the type I one enhances the carrier recombination. Generally, the recombination mechanisms for halide perovskites and the related heterojunctions can be described below:

$$\frac{dn}{dt} = G - k_1 n - k_2 n^2 - k_3 n^3 \quad (1)$$

where G (cm^{-3} s^{-1}) is the generation rate, and k_1 (s^{-1}), k_2 (cm^3 s^{-1}) and k_3 (cm^6 s^{-1}) are monomolecular, bimolecular, and Auger recombination rates, respectively. Among them, k_2 and k_3 are the intrinsic parameters for the semiconductor, and k_1 is an extrinsic factor that can evolve with the defect and doping densities.[12] The carrier recombination can be classified as either radiative or non-radiative recombination. The former will benefit both the photoelectric conversion and the light-emitting properties, while the latter is often inevitable but could compromise the device performance.[91,92]

Among the widely explored strategies for regulating charge carrier transport or recombination within halide perovskites, forming the heterojunction provides a promising way to enhance or alleviate the light-emitting property. To enhance the radiative recombination for high-performance light-emitting devices, both

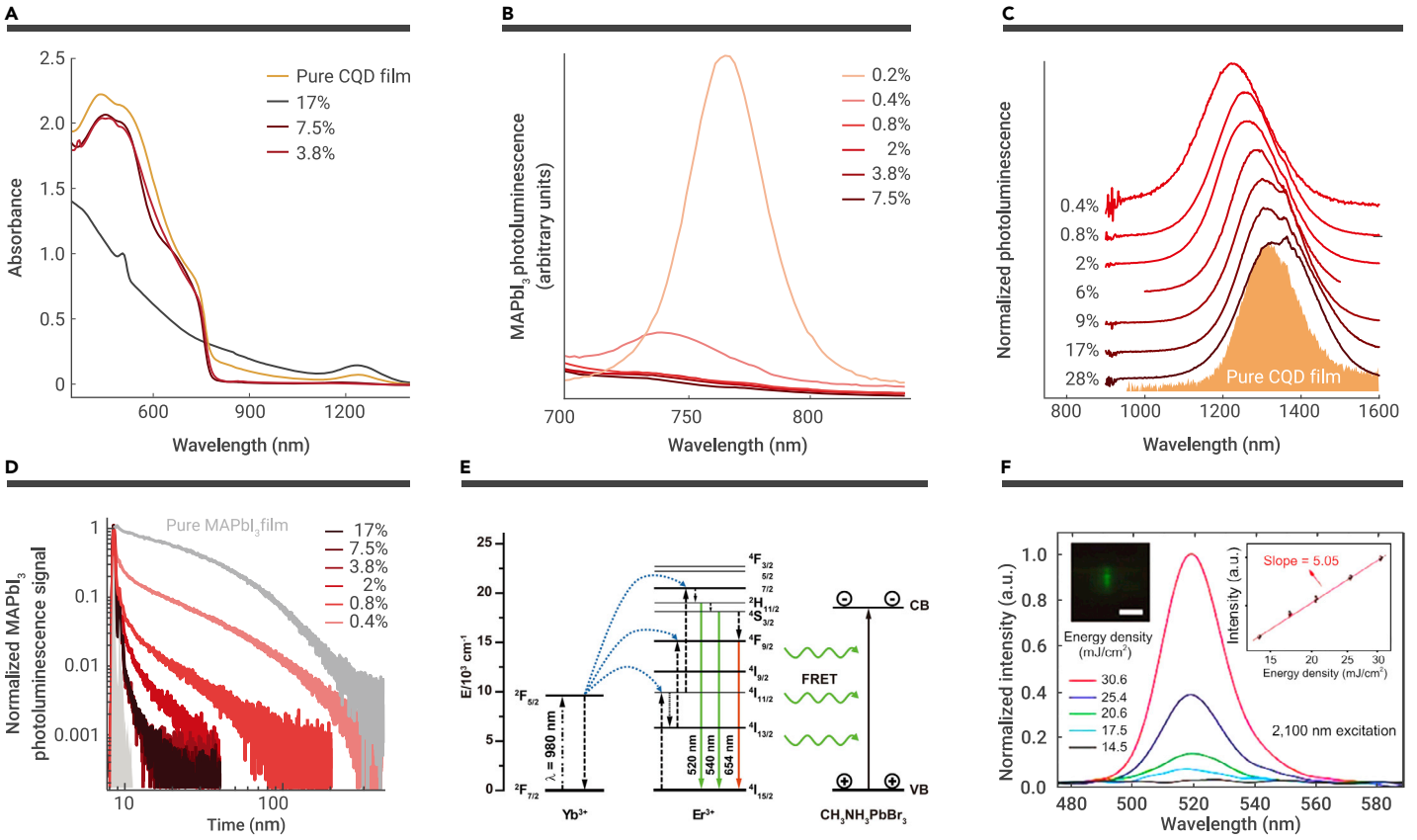

Figure 4. Optical properties for perovskite-based heterojunctions (A) Absorption of the PbS CQDs-in-$MAPbI_3$ matrix. (B) The dependence of PL intensity of $MAPbI_3$ on the CQD ratios. (C) The dependence of PL intensity of CQDs on the CQD ratios. (D) Time-resolved photoluminescence spectra with varying CQD ratios.[39] (A–D) Copyright 2015, Nature Publishing Group. (E) Schematic illustration of photo up-conversion through the proposed FRET process in the UCNP-perovskite composite. The photon energy stored in $2H_{11/2}$ and $4S_{3/2}$ energy levels of Er^{3+} can directly transfer to the closely conjugated perovskite through a non-radiative energy transfer process.[75] Copyright 2018, Wiley-VCH. (F) Five-photon excited luminescence of ZJU-28⊃$MAPbBr_3$ with femtosecond laser excitation at 2,100 nm. Insets: the microscopy image of a single ZJU-28⊃$MAPbBr_3$ excited at 2,100 nm (left) and emission intensity as a function of pump energy density showing the quintic dependence (right).[79] Copyright 2019, Wiley-VCH.

the organic polymers and small molecules have been explored.[93–96] The perovskite/polymer heterojunctions showed greatly improved light-emitting properties compared with the pure perovskites. Transient absorption measurements suggested that the localized higher-energy excitons quickly dissociated into charge carriers at lower-energy sites before energy tunneling or non-radiative recombination happened. Perovskite/polymer heterostructures also exhibited a longer lifetime and lower trap densities than those of the pure perovskite single crystals. Non-radiative relaxation processes at both the bulk and interface were effectively suppressed, leading to the excellent EQEs and near-unity external PLQEs.[96] With the compatible functional groups, such as amino, carboxyl, hydroxyl, Lewis acids or bases, small organic molecules are also widely explored for defect passivation in perovskite-based heterojunctions through forming hydrogen bonds, coordination bonds, or ionic bonds.[37,44,97–99]

Nonlinear optical properties

The rich structural and chemical diversity of halide perovskites, together with their tunable bandgap and large optical oscillator strength, have made them promising candidates for the second-, third-, and higher-order nonlinear optical (NLO) device applications.[100,101] The formation of perovskite/semiconductors heterojunctions may cause or enhance their nonlinear optical properties in several aspects[101]: (1) the second-order nonlinearity needs asymmetry, and most halide perovskite is symmetric, so it is difficult to excite the second-order nonlinear effect. The introduction of heterojunction can break the symmetry and stimulate the second-order nonlinear effect.[102] (2) The energy transfer between heterojunctions can be realized to adjust the light emission wavelength. For example, by introducing 2D/3D perovskite heterojunctions, the second-order nonlinear coefficient can be effectively improved.[103] (3) The mixed-component heterojunction effectively improves the up-conversion efficiency.[85,104] Bulk halide perovskites may work as triplet sensitizers to enable the triplet-triplet annihilation-based photon up-conversion mechanism.[104] (4) The stability of perovskite nonlinear devices can be effectively improved by introducing stable components into heterostructures.[63,105]

Light up-conversion and down-conversion can also be achieved via constructing the perovskite-based heterojunctions.[106–108] The up-conversion materials have distinctive characteristics, such as large anti-Stokes shift and NIR-light-excitable and emission-tunable features. As an example, by introducing lanthanide (La)-doped up-conversion nanoparticles (UCNP) into $CH_3NH_3PbBr_3$ perovskite nanowires, the photo-response ranging from visible to NIR light was achieved through Förster resonance energy transfer (FRET), with an achieved efficiency of 28.5% (Figure 4E).[75] Ruan et al. mixed the hexagonal-phase $NaYF_4$ UCNPs with the cubic-phase $CsPbBr_1X_2$ PQDs in heterostructured bi-phase NCs, leading to efficient FRET from the UCNP to the QD under NIR light illumination.[105] In addition, by further tuning the lattice matching between the PQDs and UCNP with Gd, the optimized $CsPbBr_3$-$NaGdF_4$:Yb,Tm NCs showed the much-enhanced luminescence up-conversion and stability.[43] This strategy of combining PQDs and UCNPs to form heterojunctions by reducing the crystal lattice mismatch to achieve enhanced FRET and stability could also improve the structure and PL stability.[105,107] Higher-order multiphoton-excited (MPE) up-conversion single microcrystalline materials are fundamentally and technologically important, but are very rare. The heterojunction formed between metal-organic-framework (MOF) and PQDs was reported to realize up to five-photon excited luminescence, as shown in Figure 4F. Such a strategy has many advantages, including a high QD loading concentration, significantly diminishing aggregation-caused quenching effect, providing effective surface passivation, and protecting QDs from the external environments due to the confinement effect of the framework.[79] As down-conversion materials, PQDs also have potential applications in photodetection and display.[76,109] For example, Cs_4PbBr_6 in the two-phase inorganic perovskite material ($CsPbBr_3$–Cs_4PbBr_6) can be used as a light

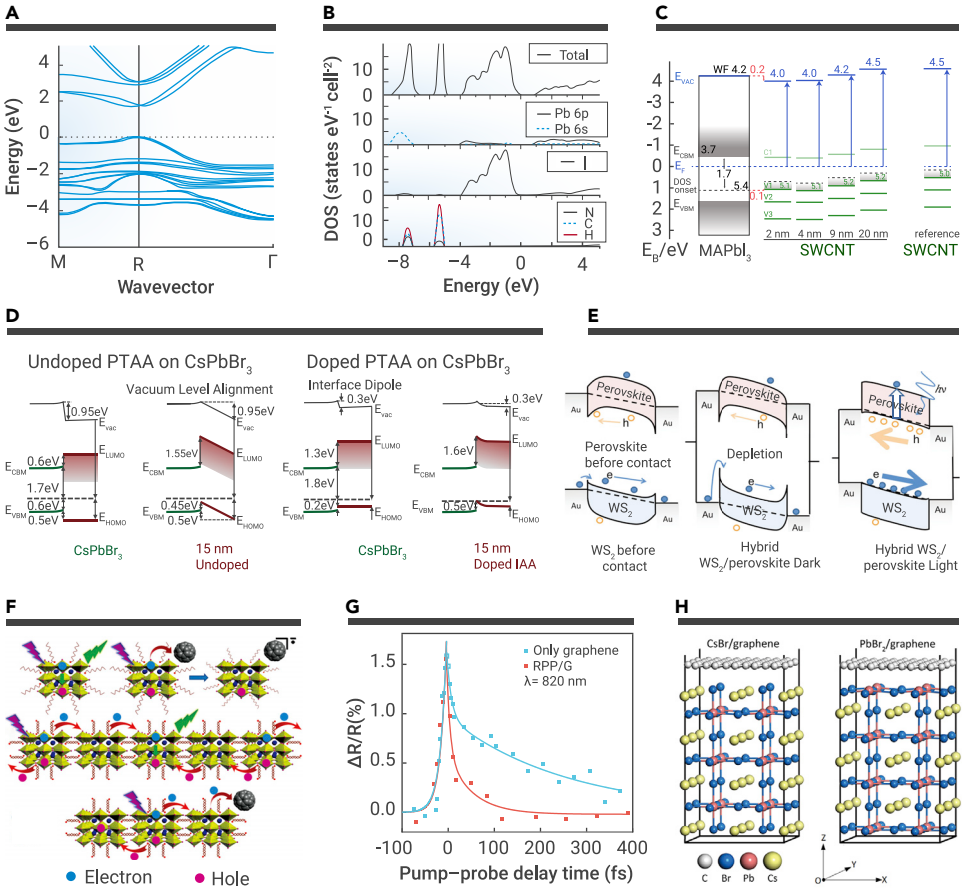

Figure 5. Electronic structures and properties of perovskites and heterojunctions (A) Band structure of cubic-phase $MAPbI_3$ calculated with the many-body perturbation theory in the GW approximation.[115] Copyright 2016, Nature Publishing Group. (B) Projected density of states (DOS) of tetragonal-phase $MAPbI_3$ (calculated with semi-local DFT) showing elemental contributions to each band.[116] Copyright 2014, American Physical Society. (C) Energy-level diagram between perovskite and SWCNTs. Values for the work function (WF) are denoted in blue, electron affinity and ionization energy of the $MAPbI_3$ layer are denoted in black, and ionization energies of the SWCNT layer are denoted in green.[117] Copyright 2016, American Chemical Society. (D) Band diagrams showing the possible energy-level alignment at the $CsPbBr_3$ interface with undoped PTAA and doped PTAA. The left diagrams assume vacuum level change are only due to an interfacial dipole. The right diagrams assume the vacuum level alignment at the interface and molecular level "bending" in the PTAA layer.[118] Copyright 2017, American Institute of Physics. (E) Proposed working mechanism of the perovskite/WS_2 bilayer photoconductor. (Left) Before contact; (middle) contact in dark; (right) contact with the light illumination.[64] Copyright 2016, Wiley-VCH. (F) Schematic presentation of exciton dynamics in photoactivated $FAPbBr_3$ /C60 composites. Top, fluorescence of perovskite and electron transfer to C60 in a solution; middle, exciton migration in a perovskite film; bottom, trapping of migrating exciton by C60 doped in a perovskite film.[114] Copyright 2017, Wiley-VCH. (G) Femtosecond pump-probe study of dynamic photocarrier injection across Ruddlesden-Popper perovskite/G heterostructure. Cross section of the data plotted at λ = 820 nm for $FAPbBr_3$ perovskite/C60 composites. Solid lines in the graph correspond to fits considering exponential growth (t < 0 fs) and decay (t > 0 fs) functions.[119] (G and H) Copyright 2020, Nature Publishing Group. (H) Theoretical optimized CsBr/graphene and $PbBr_2$/graphene interfaces. The Cs, Pb, Br, and C atoms are labeled by yellow, pale red, blue, and gray colors, respectively.[120] Reproduced with permission. Copyright 2020, American Chemical Society.

capture layer to down-convert shortwave light to achieve faster and more sensitive photoelectric detection in the deep ultraviolet (DUV) spectrum.[76]

ELECTRONIC STRUCTURE AND CARRIER TRANSPORT PROPERTIES

Electronic transport property lies at the core of high-performance perovskite optoelectronics. The formation of heterojunction between halide perovskite and other semiconductors will change the electronic properties, including trap density, band alignments, carrier transport, and recombination routes, and provide more possibilities and interesting phenomena.[91,110–114] The band structure of the commonly used cubic $MAPbI_3$ is shown in Figure 5A, which presents the basic electronic structural features of this prototype perovskite material in the original unit in its ideal structure. The band structure was calculated by using the many-body perturbation theory in the GW approximation, including spin-orbit coupling, which is the theoretical state-of-the-art method for obtaining the band structure.[91,115] According to these calculations, combined with the experimental results, the fundamental bandgap of $MAPbI_3$ can be obtained to be about 1.6~1.7 eV. The cubic $MAPbI_3$ is a direct-gap semiconductor; i.e., the valence band maximum (VBM) and conduction band minimum (CBM) appear at almost the same point in the Brillouin zone. The tetragonal- and orthorhombic-phased $MAPbI_3$ perovskites are also semiconductors that have direct fundamental bandgaps.[91] These suggest that, in $MAPbI_3$ perovskite, light absorption can proceed without phonon assistance. With the introduction of additional components, the properties, including carrier distribution, defect state density, energy band structure, transport properties, and PL, of the composited matrix will be changed accordingly. The projected density of states (DOS) of the tetragonal $MAPbI_3$ calculated with semi-local DFT is shown in Figure 5B, which shows the contribution of each element to the band structures of perovskites.[91] The conduction band consists mostly of Pb states, while the valence band consists primarily of I states with some admixture of Pb states. Given the high diversity of halide perovskites and other semiconductors, their electronic properties can be tuned in a wide range, including electronic band structures, charge transport and scattering mechanism, recombination process, and immigration.

Electronic band structures within heterojunctions

As mentioned above, halide perovskites with various compositions or dimensions can form heterojunctions with other functional semiconductors, including QDs, 1D and 2D materials, and organic semiconductors. Single-walled carbon nanotubes (SWCNTs) exhibit unique electronic properties, including tunable band alignments, as well as the atomic, molecular, and ionic functionalized covalent or noncovalent bonds. The SWCNTs can show electrical transport behaviors ranging from metallic behavior, to degenerately doped semiconductors with zero bandgap, to true semiconductors with diameter-tunable bandgaps. The electronic energy-level alignment at the $MAPbI_3$/SWCNT interface leads to the unique charge transfer process between them, as shown in Figure 5C.[117] Transient absorbance measurements show that the ground-state charge transfer at the interface would facilitate the photo-excited charge transfer in the vicinity of this junction and thus hinder recombination. Electron donation appears to be potentially from the MA group of hybrid perovskites to the contacted SWCNTs, resulting in the interfacial dipoles and the n-doped SWCNTs directly adjacent to the perovskites. Such a process or a similar mechanism is speculated to stabilize the $MAPbI_3$ perovskite surface, thus leading to more resilient devices.[117] Further investigation indicated that applying electric fields could also modify the heterostructure types with different band alignments (even the type III band alignment can be obtained in the $MAPbI_3$/CNTs heterojunction).[42] CNTs have high carrier mobilities, which may closely interact with the perovskites and fasten the transport of photo-induced charge carriers, thus significantly improving the overall mobilities of the devices. Notably, various scattering mechanisms, particularly coulomb scatterings from the trapped charges, could have detrimental effects on the charge carrier mobilities. In this regard, the scattering mechanisms need to be considered when designing the heterojunctions. For the perovskite/CNT composite-based transistors, electrons and holes would be separated in the composited channel, due to the type II interface band alignment, so that the coulomb scatterings between the photo-induced carriers are significantly suppressed, which may lead to superior carrier mobility.[121]

Band alignments at the interface between $CH_3NH_3PbI_3$ perovskite and semiconducting polymers play a key role in designing various optoelectronic

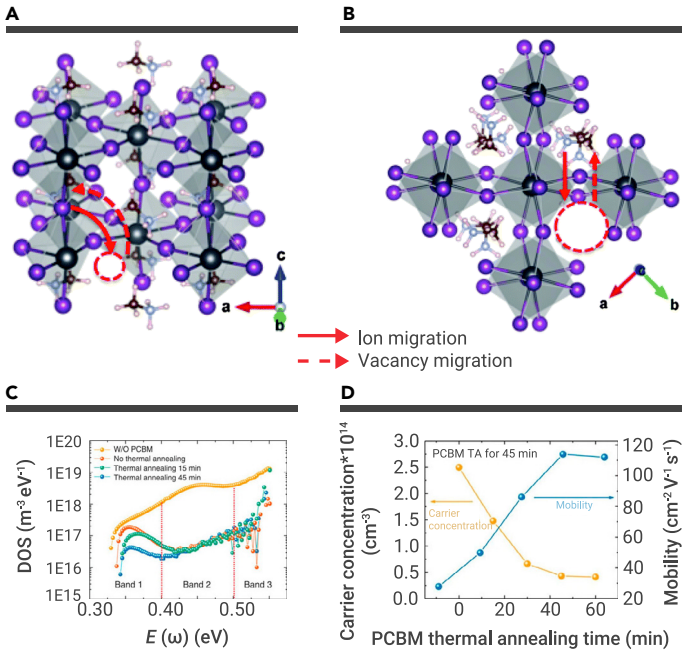

Figure 6. The effect of ion and vacancy migrations on perovskite heterojunctions (A and B) (A) Diffusion paths for the V_I defect and (B) V_{MA} defect. Vacancies are highlighted with dashed circles. Red atoms refer to interstitial defects. Solid lines stand for the migration of the ions, whereas dashed lines indicate the trajectory of the vacancy. White, H; brown, C; blue, N; purple, I; and black, Pb atoms.[139] (A and B) Copyright 2015, Royal Society of Chemistry. (C) Trap DOS (t-DOS) obtained by thermal admittance spectroscopy. t-DOS for devices without PCBM (orange), with PCBM but no thermal annealing (red), with 15-min thermal annealing PCBM (green), and 45-min thermal annealing PCBM (blue). (D) Electronic properties of perovskite films without PCBM and with varied PCBM thermal annealing time.[97] (C and D) Copyright 2014, Springer Nature.

devices.[70,71,118,122–126] James et al. exploited the stability for band alignment between all-inorganic perovskites and carrier-selective organic interlayers (Figure 5D). Using UV, X-ray, and inverse photoemission spectroscopy measurements, the ionization energy and electron affinities of both the perovskite $CsPbBr_3$ and the hole transport polymer polytriarylamine (PTAA) were obtained, which showed that PTAA could introduce a barrier of 0.2–0.5 eV for the hole extraction, due to the band bending in the PTAA and/or the dipoles at the interface. In contrast, the *p*-doped PTAA could eliminate the barrier, which would raise the highest occupied molecular orbital (HOMO) of PTAA to the level that is 0.2 eV higher than the VBM of $CsPbBr_3$, thus improving the hole transport within the system.[118]

CQDs offer an additional choice for designing the well-defined perovskite-based heterostructures, due to their nanometer-scale limited effect, discrete atom-like electronic structure, and size-dependent energy levels.[31,39] As the bandgaps of perovskites can be easily tuned via changing the halide ions, both the type I and type II heterojunctions containing perovskites and QDs can be obtained. For example, based on the band alignments, the $CsPbBr_3/ZrO_2$ NCs could be assigned as the type I composites, whereas the $CsPbI_3/ZrO_2$ NCs could be indexed as the type II composites.[31]

Carrier mobility and scattering mechanisms

The charge transport properties of halide perovskites and the scattering mechanisms are of pivotal importance for perovskite optoelectronics.[114,127,128] The effective semiconductor mobility μ_{eff} is limited by different scattering parameters, which can be approximated by the Matthiessen's rule:

$$\frac{1}{\mu_{eff}} = \frac{1}{\mu_{impurity}} + \frac{1}{\mu_{phonon}} + \frac{1}{\mu_{defect}} \quad (2)$$

where $\mu_{impurity}$, μ_{phonon}, and μ_{defect} are the individual mobilities that are limited by Coulombic interactions with impurities, phonon scattering with lattice, or surface or bulk defects, respectively. The introduction of carriers and/or ionized impurities from the added semiconductor may affect μ_{eff} by changing the different scattering mechanisms.[12] As the carrier mobilities of halide perovskites are lower than these of the traditional semiconductors, such as GaAs and Si crystals,[129] combining perovskites with the high-mobility functional materials is highly attractive. The obtained heterojunctions would take advantage of the high carrier mobilities of materials involved and the large light absorption coefficients, long exciton diffusion length, and low exciton binding energy of perovskites to improve device performance greatly.[43] For instance, heterostructures combining halide perovskites with various 2D materials, such as graphene,[119] MoS_2,[130,131] WS_2,[64,132] and WSe_2,[133] have been explored for high-performance optoelectronic devices. As for the low-dimensional perovskite cases, to resolve the major bottleneck of the high charge transport barrier within quasi-2D perovskite caused by organic molecular layers on its basal plane, the graphene/2D perovskite heterojunctions offer a lower barrier for charge carrier injection than using gold. The electron tunneling phenomenon across the interface would appear via a direct tunneling-to-field emission mechanism, which makes it possible for the charge transfer at the femtosecond timescale (~50 fs).[119] Significantly, the theoretical calculations suggest that an intrinsic built-in electric field, pointing from graphene toward the $CsPbBr_3$ layer, can promote the separation of photo-induced charge carriers at the $CsPbBr_3$/graphene interface and simultaneously inhibit the recombination of electron-hole pairs.[134] The perovskite/MoS_2 heterojunction can significantly suppress the recombination of photo-generated charge carriers, due to the selective electron trapping in MoS_2 nanoflakes, while the photo-induced hole transfer from perovskites to WS_2 and rGO in the related heterojunctions can facilitate the large increase of photocurrent. Figure 5E shows the band bending cases before and after perovskite/WS_2 heterojunction is formed.[64] Efficient interfacial charge transfer from the perovskite $CsPbBr_3$ layer to the WS_2 side was also confirmed. Some small organic molecules such as fullerene can also accelerate the formation of excitons and the transfer of electrons, thus enhancing the solar cell performance. Adding the organic small molecule C60 into a solution of perovskite may also result in the quantitative quenching of perovskite fluorescence, but without any change to the fluorescence lifetime. Such a static quenching of fluorescence is credited to efficient electron transfer from perovskite to C60. The schematic exciton dynamics in the perovskite/C60 heterojunctions are shown in Figure 5F.[114]

Once halide perovskites are combined with 2D materials, highly enhanced charge transfer can be obtained because of the overlap of the *p*-orbital electron clouds of halide perovskites and 2D materials. Figure 5G displays the dynamic photocarrier injection across PQD/graphene heterojunction through the femtosecond pump-probe study. The devices exhibited high performances for the phototransistors (PTs) and photonic synapses. The reason may lie in the fact that the graphene/PQDs superstructures could synchronize the efficient charge carrier generations and transports within a single platform.[135] Such strategy works not only for devices based on the PQDs but also for those based on multi-dimensional perovskites, such as single crystals.[136] It is worth mentioning that the crystal faces and surface functional groups of the heterojunction interface are important for the charge transfer. The $CsPbBr_3$/graphene heterostructures have two different types of interfaces, which are CsBr/graphene and $PbBr_2$/graphene (Figure 5H). The optical conductivity of the $PbBr_2$/graphene heterostructure is superior to that of the CsBr/graphene heterostructure in the infrared and visible ranges, which can be explained by the band bending, stronger built-in electric field, and lower effective mass.[120]

Ion migration and hysteresis

Mixed ion/electron transport is a ubiquitous and significant feature of metal halide perovskites. Understanding and controlling the ion transport process in perovskite materials has been a formidable challenge, and it is the key to the development of state-of-the-art perovskite devices.[137] Ion migration could bring a series of consequences, such as hysteresis, degradation, phase separation, or ionic conduction, for the related devices. By introducing another semiconductor into perovskite, the ion motion and other properties of the perovskite/semiconductor composited matrix will be changed accordingly.[113]

The ion migration may lead to defects, and the most likely defects are vacancies and interstitials due to their low formation energies.[138] Iodine and MA vacancies have low activation energies of 0.08 and 0.46 eV, respectively. In $MAPbI_3/TiO_2$ heterojunctions, the iodine and MA vacancies can easily diffuse and move in perovskite crystals according to the first-principles computational analysis (Figures 6A and 6B).[139] Under the operating conditions, iodine-related

defects are expected to migrate to the electrodes within an extremely short timescale (<1 μs), and, at the perovskite/TiO_2 interface, the negatively charged defects such as MA vacancies close to the electron transport layer (i.e., TiO_2) could change the electronic state of the perovskite and hinder charge extraction at selective contacts, resulting in the reduced hysteresis effect in the related devices.[139] The ion migration and the hysteresis effect may thus be mitigated after forming the perovskite-based heterojunction. Small molecules such as phenyl-C_{61}-butyric acid methyl ester (PCBM), or CQDs can effectively suppress the ion migration and eliminate the photocurrent hysteresis in the devices based on perovskite films due to its passivation effect.[65,140,141] Figure 6C indicates that either deep traps or shallow traps could be passivated via perovskite/PCBM heterostructures. The significant reduction in trap DOS (t-DOS) is consistent with the reduction in the photocurrent hysteresis. Figure 6D shows the changes in the carrier concentration and mobility as the PCBM thermal annealing duration increases from 15 min to 1 h. After 45 min of annealing, the hole mobility could be increased up to 114 $cm^2\ V^{-1}\ s^{-1}$.[97]

Ion migration within halide perovskites has also sparked considerable interest in the electrically stimulated artificial synapses. Synapses integrate information transmission and data storage, and thus can greatly improve the computing speed.[142,143] In a perovskite synapse, electrical pulses drive migration of ions. When the pulse amplitude is low and the pulse number is small, some ions just move in a short distance then quickly return to their positions. This process underlies the mechanism of short-term plasticity. The perovskite/semiconductor heterojunctions will affect ionic migration, cause redistribution of ions across the material, and tune the memristive behaviors.[144] Hao et al. demonstrated that the type II band offset between (6,5) s-SWCNTs and perovskite NCs enabled the photo-generated hole injection from perovskite NCs into s-SWCNT channels, leading to high memory and neuromorphic performance. The mechanism for the device performance improvements can be ascribed to the quantum gain effect.[112] Pradhen et. al. demonstrated ultrathin phototransistors and photonic synapses using a PQD/graphene heterostructure synchronize efficient charge generation and transport on a single platform. The light-assisted memory effect of these superstructures enables photonic synaptic behavior, where neuromorphic computing is demonstrated by facial recognition with the assistance of machine learning.[135]

PHOTOSTABILITY AND MECHANICAL PROPERTIES

Photostability

The photostability of halide perovskite materials is a substantial challenge for their applications and commercialization.[145] The formation of perovskite/semiconductor heterostructures may help to improve the photostability following several mechanisms:

(1) Inhibiting material decomposition by charge transfer. The photo-generated reactive oxygen species (O^{2-}) could cause rapid decomposition of perovskites by the deprotonation of organic cations.[146] The perovskite/semiconductor heterojunctions can facilitate the rapid transfer of the photo-generated charge carriers, thus avoiding the perovskite decomposition induced by carrier accumulation. SWCNTs,[117,147] small molecules,[97,114,148] and 2D materials[149–151] are all promising candidates for improving perovskite stability and charge transporting property.

(2) Steric hindrance effect. The formation of perovskite/semiconductor heterostructures can physically block the penetration of water and oxygen into the perovskite, thus improving their photostability.[148] Both perovskite/C60 planar heterostructure[97,152] and the perovskite/CNT bulky heterostructures have shown improved stability due to the high crystallinity and absence of grain boundary.[153] The heterojunctions can affect the crystallographic orientation and inhibit the phase separation, thus avoiding decomposition caused by light, thermal, and other stimuli.[2,41,154]

(3) Hindering the ion migrations. The interaction force between the halide perovskites and the semiconductor materials, such as ionic bonds and hydrogen bonds, can effectively immobilize the perovskite component in the lattice to enhance the overall stability. Small molecules such as PCBM has been reported to effectively suppress ion migration and suppress photocurrent hysteresis, thus improving their photostability.[97] The 2D perovskite/CNT heterostructure could also influence the ion migration characteristics in the transistors through the photogating effect, thus realizing the function of photomemory with enhanced device stability.[112]

Mechanical properties

The intrinsic instability issues have restricted perovskite from large-scale commercialization. Being different from traditional semiconductors, the elastic constants of halide perovskites are remarkably low, and the intrinsic mechanical properties of halide perovskite are unstable.[155–162] As for the commonly used iodine perovskites such as $MAPbI_3$ and $FAPbI_3$, their elastic constants were calculated to be 21.8 and 11.1 GPa for the elastic constant C_{11}, 7.3 and 2.7 GPa for C_{44}, and 11.3 and 5.5 GPa for C_{12}, respectively.[163] While the values of brominated perovskites have slightly larger elastic constants than the iodine ones, they are still much lower than traditional semiconductors (on the order of 102 GPa).[164,165] Recently, the model of elastic properties for the approximation of perovskite materials has been developed, which could be used to estimate the lattice distortions and to explain the experimental observations.[166] For example, strain relaxations in halide perovskite can be realized through octahedra rotations (opposite variations of in-plane and out-of-plane lattice parameters) rather than bond stretching, as is the case in traditional semiconductors.[18] The concept of coherent interfaces with lattice mismatch developed in this model also provides simple rules for the design and growth, which reveals that the structural dynamics and lattice softness can affect the physical properties. The origin of the lattice softness of halide perovskites could result in their poor lattice stability.[167] Goldschmidt tolerance factor (t) is used to predict the stable crystal structures of perovskite materials. $t = (R_A + R_X)/[\sqrt{2}(R_B + R_X)]$, where R_A, R_B, and R_X are the ionic radii of the corresponding ions, respectively. Halide perovskites tend to form an ideal cubic structure when $0.8 < t < 1$, an orthorhombic structure when $t < 0.8$, and a hexagonal structure when $t > 1$.[168,169] The lattice softness and flexibility of halide perovskites makes them difficult to guarantee its certainty in the growth process.[170]

The perovskite/semiconductor heterostructures can effectively improve the mechanical stability of halide perovskites by synergy effect. The flexible polymer substrate can effectively reduce the lattice stress of perovskites and improve their mechanical stability.[160] Chang et al. utilized conducting polymer with a large amount of Lewis base functional groups to passivate the defects and vacancies created by under-coordinated Pb atoms, which enabled the optimized perovskite film with superior stability and excellent optoelectronic properties.[155] Zhou et al. employed a novel polyethylenimine (PEI)-modified cross-stacked super-aligned CNT film in the inverted planar perovskite solar cells. Suitable energy-level alignment, promoted interfacial charge transfer, and high mechanical strength of CNTs enabled highly efficient solar cells with high stability.[171] Since the lattice stability of SnO_2 layer is much higher than that of perovskite, a perovskite/SnO_2 heterojunction can not only improve the mechanical stability of halide perovskite[161] but also form a compact oxygen and water barrier, significantly improving the environmental stability of the devices.[162,172]

DESIGN OF HETEROSTRUCTURES ON DEMAND

Highly efficient perovskite devices desire rationally designed heterostructures, which can provide benefits including enhanced stability, suppressed ion migration, and abundant catalytic active sites to drive chemical reactions (Figure 7). To achieve the goals, several parameters should be considered, such as the material properties, processability, and feasibility. The type I heterostructure may benefit radiative recombination, suppress Auger recombination and non-radiative recombination, and thus helps improve the light-emitting efficiency of LEDs. The type II heterostructure may help broaden light absorption and improve charge transport and collection efficiency, thus improving device performance and stability. This can be utilized for solar cells, PDs, PTs, and photocatalysis (PC). The roles of perovskite-based heterojunctions in various devices will be briefly discussed next.[92,172–178]

Solar cells

Solar cells are the key device application for halide perovskites. For these devices, the conversion efficiency may be calculated using the following formula:

$$\eta = \eta_{ab} \times \eta_{se} \times \eta_{tr} \times \eta_c \quad (3)$$

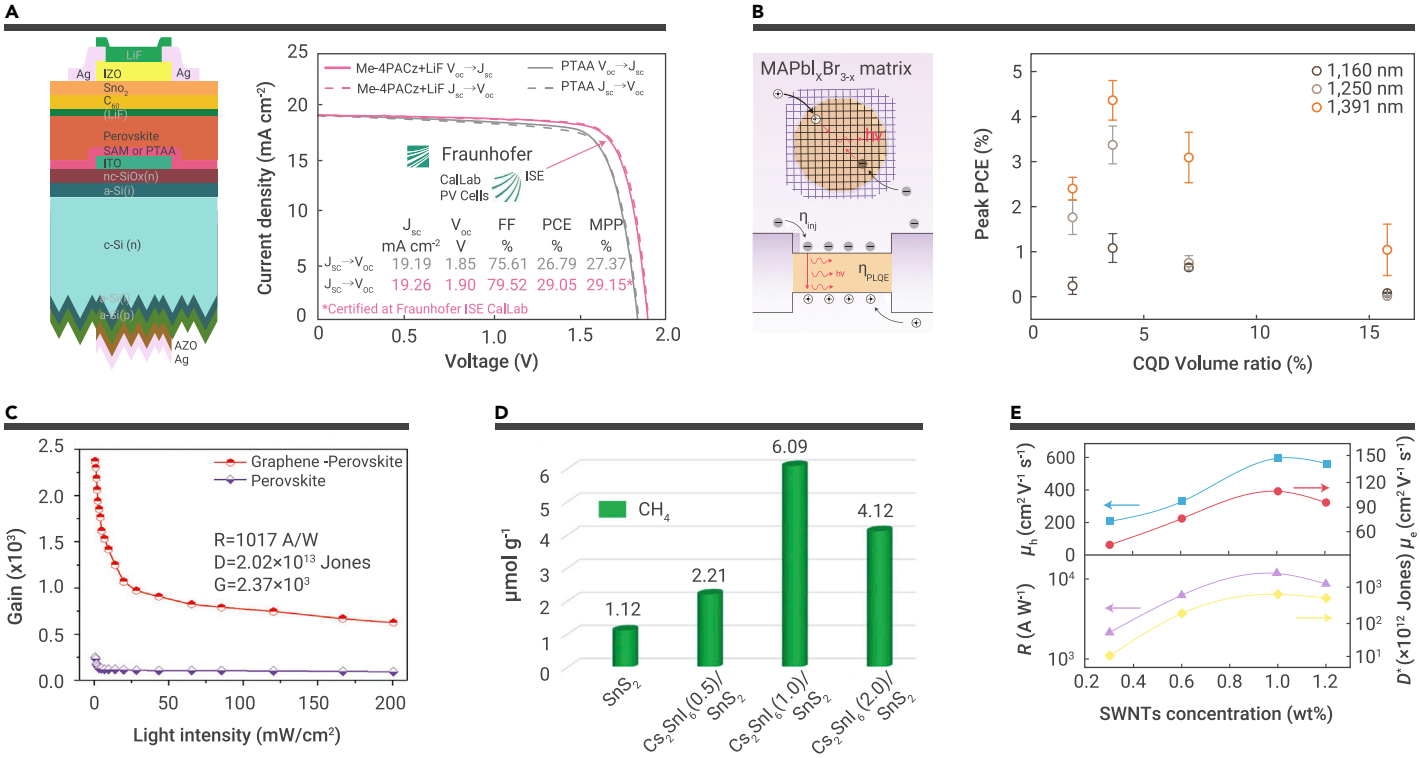

Figure 7. The applications based on the perovskite heterojunctions (A) Schematic stack of the monolithic perovskite/silicon tandem solar cell and the certified J-V curve measured at Fraunhofer ISE, including the maximum power point (MPP) value and the device parameters (red), compared with a tandem cell with PTAA (gray) as hole transporting layer.[46] Copyright 2020, American Association for the Advancement of Science. (B) (Left) Illustration of enhanced electroluminescence efficiency in PbS QDs in $MAPbI_xBr_{3-x}$ perovskite CQD LEDs, the left panel illustrates that radiative recombination dominates when QDs and perovskite are lattice matched. (Bottom) The corresponding spatial band diagram shows the mechanism of carrier transport, injection, and recombination. (Right) Average peak PCE values of QD-in-perovskite devices with various perovskite/CQD volume ratios and device emission wavelengths. Error bars represent the standard deviation of several devices.[59] Copyright 2016, Nature Publishing Group. (C) The gain of photodetectors based on $MAPbBr_3$ and $MAPbBr_3$/graphene heterostructure under 532-nm illumination.[136] Copyright 2020, Wiley-VCH. (D) Comparison of photocatalytic CO_2 reduction activities of SnS_2, $Cs_2SnI_6(0.5)/SnS_2$, $Cs_2SnI_6(1.0)/SnS_2$, and $Cs_2SnI_6(2.0)/SnS_2$.[179] Copyright 2019, American Chemical Society. (E) Effect of the CNT concentration on the performance of the hybrid perovskite/CNT phototransistor. μ_h, μ_e, R, and D^* denote hole mobility, electron mobility, responsivity, and detectivity, respectively.[121] Copyright 2017, Wiley-VCH.

where η_{ab} is the absorption efficiency, η_{se} is the separation efficiency, η_{tr} is the transport efficiency, and η_c is the efficiency of charge collection. The heterojunctions have played a significant role in improving charge carrier generation, transfer, transport, or collection, thus attracting lots of attention. For solar cells with a single-layer perovskite as the active layer, the heterojunctions may contribute in several aspects. For example, low-bandgap polymers may also help enhance light absorption in the NIR region, broadening the photo-response range with improved mechanical durability, which makes the device suitable for flexible and wearable applications.[180] Meng et al. introduced a conjugated polymer (PTQ10) as an interfacial layer in perovskite solar cells, which can precisely control the stoichiometric balance and ionic defects of perovskite surface properties.[41] The addition of polymers with thermal annealing significantly reduces the loss of surface organic cations and affects the kinetics of the phase transition and the preferential orientation of the perovskite, leading to good environmental and thermal stability. Except for the conducting polymers,[96] organic small molecules,[56,181–183] CQDs,[60,77,184,185] and carbon materials[67,186] have also been employed for optimizing perovskite-based heterostructure solar cells.

Halide perovskite tandem solar cells can extend the absorption range of the single-layer devices and continuously present record power conversion efficiency (PCE) values. The fabrication technologies for the perovskite/silicon tandem solar cells have demonstrated champion PCE up to 29.1%, making a big step toward the theoretical limit of tandem devices.[46] However, halide perovskite-based composites still have some bottleneck problems, including the relatively low EQE, inappropriate contact choices, and phase instability. To resolve these problems, Albrecht's group reported monolithic perovskite/silicon tandem solar cells (Figure 7A), which could remain in the stable phase under light illumination by combining the fast hole extraction and the minimization of non-radiative recombination at the hole-selective interface.[46] Their devices could achieve a V_{OC} as high as 1.92 V and single-junction fill factor (FF) correlations up to 84%.[46] Tan's group developed all-perovskite tandem solar cells, which were constructed by stacking a mixed Br/I perovskite front cell with a wide bandgap (approximately 1.8 eV) and a mixed lead/tin (Pb/Sn) perovskite back cell with narrow bandgap (approximately 1.2 eV). A 4-trifluoromethyl-phenylammonium (CF3-PA) layer was used to enhance the passivator adsorption, which exhibited stronger perovskite-passivator interactions than the phenethyl ammonium. Such a design leads to a 26.4% PCE and could maintain more than 90% of their initial device performance after 600 h of operation at the maximum power point.[44]

LEDs

Light-emitting and displaying devices are also increasingly important application fields for halide perovskites, and much progress has been made in these fields over the past few years.[187–194] For LED devices, the device structures and key fabrication steps are like solar cells, except that the electrons and holes flow in the opposite direction within the devices and end with the radiative recombination. By rationally forming the type I heterojunction, the light-emitting properties of perovskites can be greatly enhanced.[195,196] Pure QD films have been demonstrated to suffer from a trade-off between luminous efficiency and charge transport, which results in high power consumption. By embedding QDs into hybrid perovskite matrices, the radiative recombination in perovskite/QD composites could be enhanced without increasing the turn-on voltages. Gong et al. demonstrated a record-setting NIR electroluminescence efficiency of 4.9% through making a perovskite/QDs matrix, which is over twice that of previously reported QD devices, indicating the great potential of perovskite/CQD heterojunctions in the luminescence field.[59] The illustration of PbS QDs in $MAPbI_xBr_{3-x}$ perovskite LED, corresponding spatial band diagram, and average peak PCEs are presented in Figure 7B. The formed type I band alignment could ensure that the QDs are charge acceptors and radiative emitters. The perovskite/QDs heterojunctions also showed suppressed Auger bi-exciton recombination and the bright luminescence at high excitation (600 W cm^{-2}), whereas the control materials exhibited severe bleaching.[80]

Besides CQDs, polymers can also combine perovskites and enhance radiative recombination.[97] The principles of polymer enhancing the light-emitting property of halide perovskites include (1) forming strong bonds with perovskite surfaces, (2) increasing steric hindrance to accommodate ion migration, and (3) reducing surface defects. Some small organic molecules, such as fullerene, phenethylamine, phenylalanine, and D-4-tert-butyl-Phe, have also been employed to enhance the light-emitting behaviors through passivating defects.[37,46,97,98]

Photodetectors, photocatalysis, and phototransistors

Among the three types of heterojunctions, the type II heterojunctions combining halide perovskites and other function materials can facilitate the separation of excitons, as well as the photo-induced charge carrier transport and collection, thus promoting the device applications such as photodetectors, photocatalysis, and phototransistors.[197–199] The fundamental working process of these devices consists of the following steps: (1) light absorption and exciton formation, (2) exciton diffusion, (3) charge separation, (4) charge transport, and (5) charge collection or redox reaction. Efficient charge generation, transport, and collection will enlarge the photo-generated current in photodetectors and phototransistors, or promote the photocatalytic chemical reaction.[200,201]

For PDs, the perovskite/MoS_2 heterojunction could significantly suppress the recombination of photo-generated charge carriers by selective electron trapping in the MoS_2 nanoflakes, thus largely increasing the photocurrent by transferring the photo-induced holes from perovskite to the electrode.[64,134] The vertically structured heterojunction composed of perovskite crystals and highly conductive graphene also provided an opportunity to realize the synergistic effect between perovskite and graphene, thus showing the excellent photodetector performance (Figure 7C).[136] For PC, the ultrafast photo-induced charge carrier separation between perovskite and other functional materials is also desirable.[202,203] For example, Wang et al. reported that the type II band alignment in Cs_2SnI_6/SnS_2 hybrid structures can effectively prolong the lifetime of photo-generated electrons in SnS_2, which would improve the photocatalytic performance (Figure 7D).[179]

For PTs, due to the influence of structural defects, such as grain boundaries, pinholes within the perovskite films, and the electron arrangement in lead atoms, the carrier mobility of perovskites is low.[204] Using a strategy of coupling halide perovskite with embedded SWCNTs, Li et al. significantly improved the hole and electron mobilities of perovskite-based composited films, reaching record-breaking values of 595.3 and 108.7 $cm^2 V^{-1} s^{-1}$, respectively. The synergistic effect in the composited films can be used to construct ambipolar phototransistors with ultra-high detection performance (Figure 7E).[121] Polymers, small molecules, and 2D materials are also promising candidates for producing efficient heterojunction transistors with excellent stretchable properties.[119]

CHALLENGES AND OUTLOOK

In optoelectronics, perovskite/semiconductor planar heterojunctions widely exist and the significance of interface between halide perovskites and semiconductors has been recognized. For example, in solar cells, layer-by-layer structures are widely used to construct heterojunctions. There is also increasing interest in bulk perovskite/semiconductor heterojunctions. With the help of heterojunctions, versatile structures with desirable properties can be created, including broadened absorption, promoted light emission or recombination, enhanced carrier transportation, and improved mechanical stability. The fundamental properties of perovskite may thus be modulated in a wider range. The research on perovskite/semiconductor heterojunctions is producing inspiring results. However, there are still many challenges to overcome, such as constructing more efficient optoelectronic devices and promoting the related applications. The heterojunctions are expected to provide more positive impacts on resolving these problems. We thus foresee some possible research directions that may bring more interest and fruitful outcomes in the future.

(1) From the perspective of materials, the high diversity and particularity of halide perovskite materials and semiconductor materials will provide more options for forming perovskite-based heterojunctions. The versatile properties of halide perovskite materials, including tunable compositions, structures, and dimensions, bring more opportunities for researchers from multidisciplinary communities, such as chemistry, physics, material science, and energy science. The semiconductors also offer rich options, including various compositions, structures, and properties. By adjusting the ratio of components, heterojunction types, and so forth, researchers can tune the physical properties of perovskite-based heterostructures rationally, thus pushing the frontier of research forward continuously and effectively.

(2) From the property perspective, although various optical and electrical properties of halide perovskite materials have been explored, in-depth insights on the working mechanisms of perovskite-based heterojunctions and devices are still limited. The perovskite/semiconductor heterostructures provide a platform for establishing novel working mechanisms. Wider absorption range, higher mobility, and higher luminous intensity all become possible through the synergistic effect of perovskite and semiconductors. In this regard, it is of great significance to carry out targeted investigations and leverage the synergy between perovskite and semiconductor materials to achieve breakthroughs, as shown in Table 1.

(3) From the perspective of applications, more challenges are still ahead. Taking the solar cells as an example, more effective strategies are still needed to enhance light absorption, to improve carrier transport and collection efficiencies, and thus convert more photons into charge carriers. For LEDs, rational design of the heterostructures in specific lighting wavelength with enhanced EQE is highly needed. For PTs, the synergy of high-mobility semiconductors and perovskites may lead to high-mobility devices.

In summary, we reviewed the progress on the perovskite/semiconductor heterojunctions in the past 10 years, from the perspectives of synthesis, properties, and materials, to applications for further improving the perovskite-based device performance and stability. Although some issues are not clear yet, such as defect states and phase separation, it is believed that more progress will be made in this exciting research field. Leveraging the facile fabrication technologies for perovskite-based heterojunctions, more stable and efficient optoelectronic devices can be expected, which will provide a solid platform for advancing perovskite-related research and technologies.

REFERENCES

1. Jeong, J., Kim, M., Seo, J., et al. (2021). Pseudo-halide anion engineering for α-$FAPbI_3$ perovskite solar cells. Nature ***592***, 381–385.
2. Xu, J., Boyd, C.C., Yu, Z.J., et al. (2020). Triple-halide wide–band gap perovskites with suppressed phase segregation for efficient tandems. Science ***367***, 1097–1104.
3. Dong, Y., Wang, Y.-K., Yuan, F., et al. (2020). Bipolar-shell resurfacing for blue LEDs based on strongly confined perovskite quantum dots. Nat. Nanotechnol. ***15***, 668–674.
4. Liu, A., Zhu, H., Bai, S., et al. (2022). High-performance inorganic metal halide perovskite transistors. Nat. Electron. ***5***, 78–83.
5. Younis, A., Lin, C.H., Guan, X., et al. (2021). Halide perovskites: a new era of solution-processed electronics. Adv. Mater. ***33***, 2005000.
6. García de Arquer, F.P., Armin, A., Meredith, P., and Sargent, E.H. (2017). Solution-processed semiconductors for next-generation photodetectors. Nat. Rev. Mater. ***2***, 16100.
7. Zhou, Y., Zhou, D.-D., Liu, B.-M., et al. (2016). Ultrabroad near-infrared photoluminescence from bismuth doped $CsPbI_3$: polaronic defects vs. bismuth active centers. J. Mater. Chem. C ***4***, 2295–2301.
8. Zhuang, X., Sun, R., Zhou, D., et al. (2022). Synergistic effects of multifunctional lanthanides doped $CsPbBrCl_2$ quantum dots for efficient and stable $MAPbI_3$ perovskite solar cells. Adv. Funct. Mater. ***32***, 2110346.
9. Liu, H., Wu, Z., Shao, J., et al. (2017). $CsPb_xMn_{1-x}Cl_3$ perovskite quantum dots with high Mn substitution ratio. ACS Nano ***11***, 2239–2247.
10. Haque, M.A., Li, J., Abdelhady, A.L., et al. (2019). Transition from positive to negative photoconductance in doped hybrid perovskite semiconductors. Adv. Opt. Mater. ***7***, 1900865.
11. Ren, L., Wang, Y., Wang, M., et al. (2020). Tuning magnetism and photocurrent in Mn-doped organic–inorganic perovskites. J. Phys. Chem. Lett. ***11***, 2577–2584.
12. Euvrard, J., Yan, Y., and Mitzi, D.B. (2021). Electrical doping in halide perovskites. Nat. Rev. Mater. ***6***, 531–549.
13. Righetto, M., Meggiolaro, D., Rizzo, A., et al. (2020). Coupling halide perovskites with different materials: from doping to nanocomposites, beyond photovoltaics. Prog. Mater. Sci. ***110***, 100639.
14. Peng, J., Walter, D., Ren, Y., et al. (2021). Nanoscale localized contacts for high fill factors in polymer-passivated perovskite solar cells. Science ***371***, 390–395.
15. Tan, H., Jain, A., Voznyy, O., et al. (2017). Efficient and stable solution-processed planar perovskite solar cells via contact passivation. Science ***355***, 722–726.
16. Wang, R., Xue, J., Wang, K.-L., et al. (2019). Constructive molecular configurations for surface-defect passivation of perovskite photovoltaics. Science ***366***, 1509–1513.
17. Li, M., Zhou, J., Tan, L., et al. (2022). Multifunctional succinate additive for flexible perovskite solar cells with more than 23% power-conversion efficiency. Innovation ***3***, 100310.

18. Blancon, J.C., Even, J., Stoumpos, C.C., et al. (2020). Semiconductor physics of organic-inorganic 2D halide perovskites. Nat. Nanotechnol. ***15***, 969–985.
19. Luo, Q., Ma, H., Hou, Q., et al. (2018). All-carbon-electrode-based endurable flexible perovskite solar cells. Adv. Funct. Mater. ***28***, 1870069.
20. Xu, L., Yuan, S., Zeng, H., and Song, J. (2019). A comprehensive review of doping in perovskite nanocrystals/quantum dots: evolution of structure, electronics, optics, and light-emitting diodes. Materials Today Nano ***6***, 100036.
21. Bera, S., and Pradhan, N. (2020). Perovskite nanocrystal heterostructures: synthesis, optical properties, and applications. ACS Energy Lett. ***5***, 2858–2872.
22. Guo, J., Sun, J., Hu, L., et al. (2022). Indigo: a natural molecular passivator for efficient perovskite solar cells. Adv. Energy Mater. ***12***, 2200537.
23. Hu, L., Duan, L., Yao, Y., et al. (2022). Quantum dot passivation of halide perovskite films with reduced defects, suppressed phase segregation, and enhanced stability. Adv. Sci. ***9***, 2102258.
24. Tennyson, E.M., Doherty, T.A.S., and Stranks, S.D. (2019). Heterogeneity at multiple length scales in halide perovskite semiconductors. Nat. Rev. Mater. ***4***, 573–587.
25. Duan, L., Hu, L., Guan, X., et al. (2021). Quantum dots for photovoltaics: a tale of two materials. Adv. Energy Mater. ***11***, 2100354.
26. Haque, M.A., Gandi, A.N., Mohanraman, R., et al. (2019). A 0D lead-free hybrid crystal with ultralow thermal conductivity. Adv. Funct. Mater. ***29***, 1809166.
27. Rahaman, M.Z., Ge, S., Lin, C.-H., et al. (2021). One-dimensional molecular metal halide materials: structures, properties, and applications. Small Structures ***2***, 2000062.
28. Liu, X.-K., Xu, W., Bai, S., et al. (2021). Metal halide perovskites for light-emitting diodes. Nat. Mater. ***20***, 10–21.
29. Tao, S., Schmidt, I., Brocks, G., et al. (2019). Absolute energy level positions in tin- and lead-based halide perovskites. Nat. Commun. ***10***, 2560.
30. Mao, L., Stoumpos, C.C., and Kanatzidis, M.G. (2019). Two-dimensional hybrid halide perovskites: principles and promises. J. Am. Chem. Soc. ***141***, 1171–1190.
31. Liu, H., Tan, Y., Cao, M., et al. (2019). Fabricating $CsPbX_3$-based type I and type II heterostructures by tuning the halide composition of janus $CsPbX_3/ZrO_2$ nanocrystals. ACS Nano ***13***, 5366–5374.
32. Xue, J., Wang, R., and Yang, Y. (2020). The surface of halide perovskites from nano to bulk. Nat. Rev. Mater. ***5***, 809–827.
33. Anderson, N.C., Hendricks, M.P., Choi, J.J., and Owen, J.S. (2013). Ligand exchange and the stoichiometry of metal chalcogenide nanocrystals: spectroscopic observation of facile metal-carboxylate displacement and binding. J. Am. Chem. Soc. ***135***, 18536–18548.
34. Akkerman, Q.A., Rainò, G., Kovalenko, M.V., and Manna, L. (2018). Genesis, challenges and opportunities for colloidal lead halide perovskite nanocrystals. Nat. Mater. ***17***, 394–405.
35. De Roo, J., Ibáñez, M., Geiregat, P., et al. (2016). Highly dynamic ligand binding and light absorption coefficient of cesium lead bromide perovskite nanocrystals. ACS Nano ***10***, 2071–2081.
36. Ravi, V.K., Santra, P.K., Joshi, N., et al. (2017). Origin of the substitution mechanism for the binding of organic ligands on the surface of $CsPbBr_3$ perovskite nanocubes. J. Phys. Chem. Lett. ***8***, 4988–4994.
37. Guo, Y., Apergi, S., Li, N., et al. (2021). Phenylalkylammonium passivation enables perovskite light emitting diodes with record high-radiance operational lifetime: the chain length matters. Nat. Commun. ***12***, 644.
38. Zuo, L., Gu, Z., Ye, T., et al. (2015). Enhanced photovoltaic performance of $CH_3NH_3PbI_3$ perovskite solar cells through interfacial engineering using self-assembling monolayer. J. Am. Chem. Soc. ***137***, 2674–2679.
39. Ning, Z., Gong, X., Comin, R., et al. (2015). Quantum-dot-in-perovskite solids. Nature ***523***, 324–328.
40. Imran, M., Peng, L., Pianetti, A., et al. (2021). Halide perovskite-lead chalcohalide nanocrystal heterostructures. J. Am. Chem. Soc. ***143***, 1435–1446.
41. Meng, L., Sun, C., Wang, R., et al. (2018). Tailored phase conversion under conjugated polymer enables thermally stable perovskite solar cells with efficiency exceeding 21%. J. Am. Chem. Soc. ***140***, 17255–17262.
42. Tan, Q., Wang, Q., Zhang, C., et al. (2021). Termination dependence and electric field modification of band alignment in a $CNT/CH_3NH_3PbI_3$ heterojunction. Phys. Chem. Chem. Phys. ***23***, 9249–9258.
43. Lee, G.Y., Yang, M.Y., Kim, D., et al. (2019). Nitrogen-dopant-induced organic inorganic hybrid perovskite crystal growth on carbon nanotubes. Adv. Funct. Mater. ***29***, 1902489.
44. Lin, R., Xu, J., Wei, M., et al. (2022). All-perovskite tandem solar cells with improved grain surface passivation. Nature ***603***, 73–78.
45. Zhao, D., Yu, Y., Wang, C., et al. (2017). Low-bandgap mixed tin-lead iodide perovskite absorbers with long carrier lifetimes for all-perovskite tandem solar cells. Nat. Energy ***2***, 17018.
46. Al-Ashouri, A., Köhnen, E., Li, B., et al. (2020). Monolithic perovskite/silicon tandem solar cell with 29% efficiency by enhanced hole extraction. Science ***370***, 1300–1309.
47. Wei, W., Zhang, Y., Xu, Q., et al. (2017). Monolithic integration of hybrid perovskite single crystals with heterogenous substrate for highly sensitive X-ray imaging. Nat. Photonics ***11***, 315–321.
48. Hou, Y., Aydin, E., De Bastiani, M., et al. (2020). Efficient tandem solar cells with solution-processed perovskite on textured crystalline silicon. Science ***367***, 1135–1140.
49. Kim, D., Jung, H.J., Park, I.J., et al. (2020). Efficient, stable silicon tandem cells enabled by anion-engineered wide-bandgap perovskites. Science ***368***, 155–160.
50. Kim, C.U., Jung, E.D., Noh, Y.W., et al. (2021). Strategy for large-scale monolithic Perovskite/Silicon tandem solar cell: a review of recent progress. Ecomat ***3***, e12084.
51. Liang, S., Zhang, M., Biesold, G.M., et al. (2021). Recent advances in synthesis, properties, and applications of metal halide perovskite nanocrystals/polymer nanocomposites. Adv. Mater. ***33***, 2005888.
52. Liu, Y., and Chen, Y. (2019). Integrated perovskite/bulk-heterojunction organic solar cells. Adv. Mater. ***32***, 1805843.
53. Kim, K., Han, J., Maruyama, S., et al. (2021). Role and contribution of polymeric additives in perovskite solar cells: crystal growth templates and grain boundary passivators. Sol. RRL ***5***, 2000783.
54. Li, C., Wang, H., Wang, F., et al. (2020). Ultrafast and broadband photodetectors based on a perovskite/organic bulk heterojunction for large-dynamic-range imaging. Light Sci. Appl. ***9***, 31.
55. Xie, C., You, P., Liu, Z., et al. (2017). Ultrasensitive broadband phototransistors based on perovskite/organic-semiconductor vertical heterojunctions. Light Sci. Appl. ***6***, e17023.
56. Lai, W.-C., Lin, K.-W., Wang, Y.-T., et al. (2016). Oxidized Ni/Au transparent electrode in efficient $CH_3NH_3PbI_3$ perovskite/fullerene planar heterojunction hybrid solar cells. Adv. Mater. ***28***, 3290–3297.
57. Li, Y., Dailey, M., Lohr, P.J., and Printz, A.D. (2021). Performance and stability improvements in metal halide perovskite with intralayer incorporation of organic additives. J. Mater. Chem. ***9***, 16281–16338.
58. Sun, Q., Shen, C., Wang, D., et al. (2021). Efficient and stable large-area perovskite solar cells with inorganic perovskite/carbon quantum dot-graded heterojunction. Research ***2021***, 9845067.
59. Gong, X., Yang, Z., Walters, G., et al. (2016). Highly efficient quantum dot near-infrared light-emitting diodes. Nat. Photonics ***10***, 253–257.
60. Xu, F., Meng, K., Cheng, B., et al. (2020). Unique S-scheme heterojunctions in self-assembled $TiO_2/CsPbBr_3$ hybrids for CO_2 photoreduction. Nat. Commun. ***11***, 4613.
61. García de Arquer, F.P., Gong, X., Sabatini, R.P., et al. (2017). Field-emission from quantum-dot-in-perovskite solids. Nat. Commun. ***8***, 14757.
62. Chen, H., Pina, J.M., Hou, Y., and Sargent, E.H. (2022). Synthesis, applications, and prospects of quantum-dot-in-perovskite solids. Adv. Energy Mater. ***12***, 2100774.
63. Chen, S., and Shi, G. (2017). Two-dimensional materials for halide perovskite-based optoelectronic devices. Adv. Mater. ***29***, 1605448.
64. Ma, C., Shi, Y., Hu, W., et al. (2016). Heterostructured $WS_2/CH_3NH_3PbI_3$ photoconductors with suppressed dark current and enhanced photodetectivity. Adv. Mater. ***28***, 3683–3689.
65. Zhu, Z., Ma, J., Wang, Z., et al. (2014). Efficiency enhancement of perovskite solar cells through fast electron extraction: the role of graphene quantum dots. J. Am. Chem. Soc. ***136***, 3760–3763.
66. Wang, Y., Fullon, R., Acerce, M., et al. (2017). Solution-Processed MoS_2/organolead trihalide perovskite photodetectors. Adv. Mater. ***29***, 1603995.
67. Bati, A.S.R., Yu, L., Batmunkh, M., and Shapter, J.G. (2019). Recent advances in applications of sorted single-walled carbon nanotubes. Adv. Funct. Mater. ***29***, 1902273.
68. Avery, A.D., Zhou, B.H., Lee, J., et al. (2016). Tailored semiconducting carbon nanotube networks with enhanced thermoelectric properties. Nat. Energy ***1***, 16033.
69. Luo, Q., Wu, R., Ma, L., et al. (2021). Recent advances in carbon nanotube utilizations in perovskite solar cells. Adv. Funct. Mater. ***31***, 2004765.
70. Qian, C.-X., Deng, Z.-Y., Yang, K., et al. (2018). Interface engineering of $CsPbBr_3/TiO_2$ heterostructure with enhanced optoelectronic properties for all-inorganic perovskite solar cells. Appl. Phys. Lett. ***112***, 093901.
71. Lindbad, R., Bi, D., Park, B.-w., et al. (2014). Electronic structure of $TiO_2/CH_3NH_3PbI_3$ perovskite solar cell interfaces. J. Phys. Chem. Lett. ***5***, 648–653.
72. Gao, T., Zhang, Q., Chen, J., et al. (2017). Performance-enhancing broadband and flexible photodetectors based on perovskite/ZnO-nanowire hybrid structures. Adv. Opt. Mater. ***5***, 1700206.
73. Zhang, P., Wu, J., Zhang, T., et al. (2018). Perovskite solar cells with ZnO electron-transporting materials. Adv. Mater. ***30***, 1703737.
74. Guan, X., Wan, T., Hu, L., et al. (2022). A solution-processed all-perovskite memory with dual-band light response and tri-mode operation. Adv. Funct. Mater. ***32***, 2110975.
75. Yang, B., Wang, Y., Wei, T., et al. (2018). Solution-processable near-infrared-responsive composite of perovskite nanowires and photon-upconversion nanoparticles. Adv. Funct. Mater. ***28***, 1801782.
76. Tong, G., Li, H., Zhu, Z., et al. (2018). Enhancing hybrid perovskite detectability in the deep ultraviolet region with down-conversion dual-phase ($CsPbBr_3$-Cs_4PbBr_6) films. J. Phys. Chem. Lett. ***9***, 1592–1599.
77. Zhao, C., Chen, C., Wei, R., et al. (2021). Laser-assisted synthesis of Ag_2S-Quantum-Dot-in-Perovskite matrix and its application in broadband photodetectors. Adv. Opt. Mater. ***10***, 2101535.
78. Haruyama, J., Sodeyama, K., Han, L., and Tateyama, Y. (2014). Termination dependence of tetragonal $CH_3NH_3PbI_3$ surfaces for perovskite solar cells. J. Phys. Chem. Lett. ***5***, 2903–2909.
79. He, H., Cui, Y., Li, B., et al. (2019). Confinement of perovskite-QDs within a single MOF crystal for significantly enhanced multiphoton excited luminescence. Adv. Mater. ***31***, 1806897.
80. Liu, Y., Dong, Y., Zhu, T., et al. (2021). Bright and stable light-emitting diodes based on perovskite quantum dots in perovskite matrix. J. Am. Chem. Soc. ***143***, 15606–15615.
81. Chen, S., Lyu, D., Ling, T., and Guo, W. (2018). Reversible modulation of $CsPbBr_3$ perovskite nanocrystal/gold nanoparticle heterostructures. Chem. Commun. ***54***, 4605–4608.
82. Dutta, S.K., Bera, S., and Pradhan, N. (2021). Why is making epitaxially grown all inorganic perovskite- chalcogenide nanocrystal heterostructures challenging? Some facts and some strategies. Chem. Mater. ***33***, 3868–3877.

83. Kamat, P.V., Pradhan, N., Schanze, K., et al. (2020). Challenges and opportunities in designing perovskite nanocrystal heterostructures. ACS Energy Lett. ***5***, 2253–2255.
84. Li, H., Lin, W., Ma, L., et al. (2021). High-performance broadband photodetectors based on all-inorganic perovskite $CsPb(Br/I)_3$ nanocrystal/CdS-microwire heterostructures. RSC Adv. ***11***, 11663–11671.
85. Ruan, L., and Zhang, Y. (2021). Upconversion perovskite nanocrystal heterostructures with enhanced luminescence and stability by lattice matching. ACS Appl. Mater. Interfaces ***13***, 51362–51372.
86. Sheldon, M. (2017). Hot carrier up-conversion luminescence in nanocrystal heterostructures. Abstr. Pap. Am. Chem. Soc. ***254***, 551.
87. Wong, Y.-C., De Andrew Ng, J., and Tan, Z.-K. (2018). Perovskite-initiated photopolymerization for singly dispersed luminescent nanocomposites. Adv. Mater. ***30***, 1800774.
88. de Quilettes, D.W., Vorpahl, S.M., Stranks, S.D., et al. (2015). Impact of microstructure on local carrier lifetime in perovskite solar cells. Science ***348***, 683–686.
89. Gao, L., Quan, L.N., García de Arquer, F.P., et al. (2020). Efficient near-infrared light-emitting diodes based on quantum dots in layered perovskite. Nat. Photonics ***14***, 227–233.
90. Habisreutinger, S.N., Nicholas, R.J., and Snaith, H.J. (2017). Carbon nanotubes in perovskite solar cells. Adv. Energy Mater. ***7***, 1601839.
91. Brenner, T.M., Egger, D.A., Kronik, L., et al. (2016). Hybrid organic—inorganic perovskites: low-cost semiconductors with intriguing charge-transport properties. Nat. Rev. Mater. ***1***, 15007.
92. Luo, D., Su, R., Zhang, W., et al. (2019). Minimizing non-radiative recombination losses in perovskite solar cells. Nat. Rev. Mater. ***5***, 44–60.
93. Bade, S.G.R., Shan, X., Hoang, P.T., et al. (2017). Stretchable light-emitting diodes with organometal-halide-perovskite-polymer composite emitters. Adv. Mater. ***29***, 1607053.
94. Li, J., Bade, S.G.R., Shan, X., and Yu, Z. (2015). Single-layer light-emitting diodes using organometal halide perovskite/poly(ethylene oxide) composite thin films. Adv. Mater. ***27***, 5196–5202.
95. Wang, Y., He, J., Chen, H., et al. (2016). Ultrastable, highly luminescent organic-inorganic perovskite-polymer composite films. Adv. Mater. ***28***, 10710–10717.
96. Zhao, B., Bai, S., Kim, V., et al. (2018). High-efficiency perovskite–polymer bulk heterostructure light-emitting diodes. Nat. Photonics ***12***, 783–789.
97. Shao, Y., Xiao, Z., Bi, C., et al. (2014). Origin and elimination of photocurrent hysteresis by fullerene passivation in $CH_3NH_3PbI_3$ planar heterojunction solar cells. Nat. Commun. ***5***, 5784.
98. Xu, W., Hu, Q., Bai, S., et al. (2019). Rational molecular passivation for high-performance perovskite light-emitting diodes. Nat. Photonics ***13***, 418–424.
99. Bag, M., Renna, L.A., Jeong, S.P., et al. (2016). Evidence for reduced charge recombination in carbon nanotube/perovskite-based active layers. Chem. Phys. Lett. ***662***, 35–41.
100. Wei, T., Mokkapati, S., Li, T., et al. (2018). Nonlinear absorption applications of $CH_3NH_3PbBr_3$ perovskite crystals. Adv. Funct. Mater. ***28***, 1707175.
101. Xu, J., Li, X., Xiong, J., et al. (2020). Halide perovskites for nonlinear optics. Adv. Mater. ***32***, 1806736.
102. Govinda, S., Kore, B.P., Mahale, P., et al. (2018). Can SHG measurements determine the polarity of hybrid lead halide perovskites? ACS Energy Lett. ***3***, 1887–1891.
103. Song, Y., Zhang, C., Liu, W., et al. (2018). High-efficiency energy transfer in perovskite heterostructures. Opt Express ***26***, 18448–18456.
104. VanOrman, Z.A., Drozdick, H.K., Wieghold, S., and Nienhaus, L. (2021). Bulk halide perovskites as triplet sensitizers: progress and prospects in photon upconversion. J. Mater. Chem. C ***9***, 2685–2694.
105. Ruan, L., and Zhang, Y. (2021). NIR-excitable heterostructured upconversion perovskite nanodots with improved stability. Nat. Commun. ***12***, 219.
106. Yang, L., Wei, K., Xu, Z., et al. (2018). Nonlinear absorption and temperature-dependent fluorescence of perovskite $FAPbBr_3$ nanocrystal. Opt. Lett. ***43***, 122–125.
107. Zhang, P., Liang, L., and Liu, X. (2021). Lanthanide-doped nanoparticles in photovoltaics - more than just upconversion. J. Mater. Chem. C ***9***, 16110–16131.
108. Zhou, D., Liu, D., Pan, G., et al. (2017). Cerium and ytterbium codoped halide perovskite quantum dots: a novel and efficient downconverter for improving the performance of silicon solar cells. Adv. Mater. ***29***, 1704149.
109. Lee, H., Park, J., Kim, S., et al. (2020). Perovskite emitters as a platform material for down-conversion applications. Adv. Mater. Technol. ***5***, 2000091.
110. Brauer, J.C., Lee, Y.H., Nazeeruddin, M.K., and Banerji, N. (2015). Charge transfer dynamics from organometal halide perovskite to polymeric hole transport materials in hybrid solar cells. J. Phys. Chem. Lett. ***6***, 3675–3681.
111. Liu, K., Bian, Y., Kuang, J., et al. (2022). Ultrahigh-performance optoelectronic skin based on intrinsically stretchable perovskite-polymer heterojunction transistors. Adv. Mater. ***34***, 2107304.
112. Li, Y.-T., Ding, L., Li, J.-Z., et al. (2019). Light-enhanced ion migration in two-dimensional perovskite single crystals revealed in carbon nanotubes/two-dimensional perovskite heterostructure and its photomemory application. ACS Cent. Sci. ***5***, 1857–1865.
113. Mosconi, E., and De Angelis, F. (2016). Mobile ions in organohalide perovskites: interplay of electronic structure and dynamics. ACS Energy Lett. ***1***, 182–188.
114. Nair, V.C., Muthu, C., Rogach, A.L., et al. (2017). Channeling exciton migration into electron transfer in formamidinium lead bromide perovskite nanocrystal/fullerene composites. Angew. Chem., Int. Ed. Engl. ***56***, 1214–1218.
115. Brivio, F., Butler, K.T., Walsh, A., and van Schilfgaarde, M. (2014). Relativistic quasiparticle self-consistent electronic structure of hybrid halide perovskite photovoltaic absorbers. Phys. Rev. B ***89***, 155204.
116. Du, M.H. (2014). Efficient carrier transport in halide perovskites: theoretical perspectives. J. Mater. Chem. ***2***, 9091–9098.
117. Schulz, P., Dowgiallo, A.-M., Yang, M., et al. (2016). Charge transfer dynamics between carbon nanotubes and hybrid organic metal halide perovskite films. J. Phys. Chem. Lett. ***7***, 418–425.
118. Endres, J., Kulbak, M., Zhao, L., et al. (2017). Electronic structure of the $CsPbBr_3$/polytriarylamine (PTAA) system. J. Appl. Phys. ***121***, 035304.
119. Leng, K., Wang, L., Shao, Y., et al. (2020). Electron tunneling at the molecularly thin 2D perovskite and graphene van der Waals interface. Nat. Commun. ***11***, 5483.
120. Yun, J., Fan, H., Zhang, Y., et al. (2020). Enhanced optical absorption and interfacial carrier separation of $CsPbBr_3$/graphene heterostructure: experimental and theoretical insights. ACS Appl. Mater. Interfaces ***12***, 3086–3095.
121. Li, F., Wu, T., Kufer, D., et al. (2017). Ultrahigh carrier mobility achieved in photoresponsive hybrid perovskite films via coupling with single-walled carbon nanotubes. Adv. Mater. ***29***, 1602432.
122. Vo, D.D., Idrees, M., Pham, V.T., et al. (2020). Electronic structure and optical performance of $PbI_2/SnSe_2$ heterostructure. Chem. Phys. ***533***, 110736.
123. Ji, G., Zheng, G., Zhao, B., et al. (2017). Interfacial electronic structures revealed at the rubrene/CH3NH3PbI3 interface. Phys. Chem. Chem. Phys. ***19***, 6546–6553.
124. Algadi, H., Mahata, C., Sahoo, B., et al. (2020). Facile method for the preparation of high-performance photodetectors with a GQDs/perovskite bilayer heterostructure. Org. Electron. ***76***, 105444.
125. Lo, M.-F., Guan, Z.-Q., Ng, T.-W., et al. (2015). Electronic structures and photoconversion mechanism in perovskite/fullerene heterojunctions. Adv. Funct. Mater. ***25***, 1213–1218.
126. Mardis, K.L., Webb, J.N., Holloway, T., et al. (2015). Electronic structure of fullerene acceptors in organic bulk-heterojunctions: a combined EPR and DFT study. J. Phys. Chem. Lett. ***6***, 4730–4735.
127. Bu, Y., Nam, G., Kim, S., et al. (2018). A tailored bifunctional electrocatalyst: boosting oxygen reduction/evolution catalysis via electron transfer between N-doped graphene and perovskite oxides. Small ***14***, 1802767.
128. Yang, J.-J., Liu, X.-Y., Li, Z.-W., et al. (2021). The spin-orbit interaction controls photoinduced interfacial electron transfer in fullerene-perovskite heterojunctions: C(60)versus C-70. Phys. Chem. Chem. Phys. ***23***, 6536–6543.
129. Brenner, T.M., Egger, D.A., Rappe, A.M., et al. (2015). Are mobilities in hybrid organic-inorganic halide perovskites actually "high"? J. Phys. Chem. Lett. ***6***, 4754–4757.
130. Cheng, Y., Li, H., Liu, B., et al. (2020). Vertical 0D-perovskite/2D-MoS2 van der Waals heterojunction phototransistor for emulating photoelectric-synergistically classical pavlovian conditioning and neural coding dynamics. Small ***16***, e2005217.
131. Wu, H., Si, H., Zhang, Z., et al. (2018). All-inorganic perovskite quantum dot-monolayer MoS_2 mixed-dimensional van der Waals heterostructure for ultrasensitive photodetector. Adv. Sci. ***5***, 1801219.
132. Lai, Y.-S., Del Rosario, M.A.J.V.G., Chen, W.-F., et al. (2019). Energy-yielding mini heat thermocells with WS_2 water-splitting dual system to recycle wasted heat. ACS Appl. Energy Mater. ***2***, 7092–7103.
133. Lu, J., Carvalho, A., Liu, H., et al. (2016). Hybrid bilayer WSe_2-$CH_3NH_3PbI_3$ organolead halide perovskite as a high-performance photodetector. Angew. Chem., Int. Ed. Engl. ***55***, 11945–11949.
134. Peng, Z.-Y., Xu, J.-L., Zhang, J.-Y., et al. (2018). Solution-Processed high-performance hybrid photodetectors enhanced by perovskite/MoS_2 bulk heterojunction. Adv. Mater. Interfac. ***5***, 1800505.
135. Pradhan, B., Das, S., Li, J., et al. (2020). Ultrasensitive and ultrathin phototransistors and photonic synapses using perovskite quantum dots grown from graphene lattice. Sci. Adv. ***6***, eaay5225.
136. Zou, Y., Zou, T., Zhao, C., et al. (2020). A highly sensitive single crystal perovskite–graphene hybrid vertical photodetector. Small ***16***, 2000733.
137. Zhang, T., Hu, C., and Yang, S. (2020). Ion migration: a "Double-Edged sword" for halide-perovskite-based electronic devices. Small Methods ***4***, 1900552.
138. Ding N., Wang N., Liu S., et al. (2021). Research progress on doped perovskite materials. Laser Optoelectron. P. ***58***, 1516011.
139. Azpiroz, J.M., Mosconi, E., Bisquert, J., and De Angelis, F. (2015). Defect migration in methylammonium lead iodide and its role in perovskite solar cell operation. Energy Environ. Sci. ***8***, 2118–2127.
140. Li, H., Shi, W., Huang, W., et al. (2017). Carbon quantum dots/TiOx electron transport layer boosts efficiency of planar heterojunction perovskite solar cells to 19%. Nano Lett. ***17***, 2328–2335.
141. Gatti, T., Menna, E., Meneghetti, M., et al. (2017). The Renaissance of fullerenes with perovskite solar cells. Nano Energy ***41***, 84–100.
142. Huang, X., Guo, Y., and Liu, Y. (2021). Perovskite photodetectors and their application in artificial photonic synapses. Chem. Commun. ***57***, 11429–11442.
143. Choi, J., Han, J.S., Hong, K., et al. (2018). Organic-inorganic hybrid halide perovskites for memories, transistors, and artificial synapses. Adv. Mater. ***30***, 1704002.
144. Xu, W., Cho, H., Kim, Y.-H., et al. (2016). Organometal halide perovskite artificial synapses. Adv. Mater. ***28***, 5916–5922.
145. Liang, Y., Li, F., and Zheng, R. (2020). Low-dimensional hybrid perovskites for field-effect transistors with improved stability: progress and challenges. Adv. Electron. Mater. ***6***, 2000137.
146. Fu, R., Zhou, W., Li, Q., et al. (2019). Stability challenges for perovskite solar cells. Chemnanomat ***5***, 253–265.
147. Habisreutinger, S.N., Leijtens, T., Eperon, G.E., et al. (2014). Carbon nanotube/polymer composites as a highly stable hole collection layer in perovskite solar cells. Nano Lett. ***14***, 5561–5568.

148. Heo, J.H., Im, S.H., Noh, J.H., et al. (2013). Efficient inorganic–organic hybrid heterojunction solar cells containing perovskite compound and polymeric hole conductors. Nat. Photonics **7**, 486–491.
149. Zhang, F., Park, S.Y., Yao, C., et al. (2022). Metastable Dion-Jacobson 2D structure enables efficient and stable perovskite solar cells. Science **375**, 71–76.
150. Azmi, R., Ugur, E., Seitkhan, A., et al. (2022). Damp heat-stable perovskite solar cells with tailored-dimensionality 2D/3D heterojunctions. Science **376**, 73–77.
151. Sidhik, S., Wang, Y., De Siena, M., et al. (2022). Deterministic fabrication of 3D/2D perovskite bilayer stacks for durable and efficient solar cells. Science **377**, 1425–1430.
152. Xu, J., Buin, A., Ip, A.H., et al. (2015). Perovskite-fullerene hybrid materials suppress hysteresis in planar diodes. Nat. Commun. **6**, 7081.
153. Lin, C., Lyu, Z., Zhuo, Y., et al. (2020). Microwave synthesis and high-mobility charge transport of carbon-nanotube-in-perovskite single crystals. Adv. Opt. Mater. **8**, 2001740.
154. Rehman, W., McMeekin, D.P., Patel, J.B., et al. (2017). Photovoltaic mixed-cation lead mixed-halide perovskites: links between crystallinity, photo-stability and electronic properties. Energy Environ. Sci. **10**, 361–369.
155. Chang, C.-Y., and Wang, C.-C. (2020). Enhanced stability and performance of air-processed perovskite solar cells via defect passivation with a thiazole-bridged diketopyrrolopyrrole-based π-conjugated polymer. J. Mater. Chem. **8**, 8593–8604.
156. Fu, K., He, Y., Zhang, B., et al. (2020). Enhanced aqueous stability and radiative-charge-transfer of $CsPbBr_3/Ag_2S$ perovskite nanocrystal hybrids. J. Electroanal. Chem. **858**, 11383.
157. Huang, Y., Wang, T., Zheng, J., et al. (2021). Multiwalled carbon nanotubes/$CsPbX_3$ @Polyacrylonitrile core/shell nanofibers with ultrahigh water,. ater. Eng. **306**, 2100200.
158. Jiang, X., Zhang, J., Liu, Y., et al. (2021). Dopant-free polymer/2D/3D perovskite solar cells with high stability. Nano Energy **90**, 106521.
159. Wei, J., Guo, F., Wang, X., et al. (2018). SnO2-in-Polymer matrix for high-efficiency perovskite solar cells with improved reproducibility and stability. Adv. Mater. **30**, 1805153.
160. Wei, J., Wang, X., Sun, X., et al. (2020). Polymer assisted deposition of high-quality $CsPbI_2Br$ film with enhanced film thickness and stability. Nano Res. **13**, 684–690.
161. Zhou, Y., Yin, X., Luo, Q., et al. (2018). Efficiently improving the stability of inverted perovskite solar cells by employing polyethylenimine-modified carbon nanotubes as electrodes. ACS Appl. Mater. Interfaces **10**, 31384–31393.
162. Zhu, Z., Bai, Y., Liu, X., et al. (2016). Enhanced efficiency and stability of inverted perovskite solar cells using highly crystalline SnO_2 nanocrystals as the robust electron-transporting layer. Adv. Mater. **28**, 6478–6484.
163. Ferreira, A.C., Létoublon, A., Paofai, S., et al. (2018). Elastic softness of hybrid lead halide perovskites. Phys. Rev. Lett. **121**, 085502.
164. Vurgaftman, I., Meyer, J.R., and Ram-Mohan, L.R. (2001). Band parameters for III–V compound semiconductors and their alloys. J. Appl. Phys. **89**, 5815–5875.
165. Schmalzl, K., Schmidt, W., Raymond, S., et al. (2016). The upgrade of the cold neutron three-axis spectrometer IN12 at the ILL. Nucl. Instrum. Methods Phys. Res. Sect. A Accel. Spectrom. Detect. Assoc. Equip. **819**, 89–98.
166. Kepenekian, M., Traore, B., Blancon, J.-C., et al. (2018). Concept of lattice mismatch and emergence of surface states in two-dimensional hybrid perovskite quantum wells. Nano Lett. **18**, 5603–5609.
167. Wu, J., Liu, S.-C., Li, Z., et al. (2021). Strain in perovskite solar cells: origins, impacts and regulation. Natl. Sci. Rev. **8**, nwab047.
168. Dang, Y., Liu, Y., Sun, Y., et al. (2015). Bulk crystal growth of hybrid perovskite material CH3NH3PbI3. CrystEngComm **17**, 665–670.
169. McKinnon, N.K., Reeves, D.C., and Akabas, M.H. (2011). 5-HT3 receptor ion size selectivity is a property of the transmembrane channel, not the cytoplasmic vestibule portals. J. Gen. Physiol. **138**, 453–466.
170. Saidaminov, M.I., Kim, J., Jain, A., et al. (2018). Suppression of atomic vacancies via incorporation of isovalent small ions to increase the stability of halide perovskite solar cells in ambient air. Nat. Energy **3**, 648–654.
171. Zhou, W., Wen, Z., and Gao, P. (2018). Less is more: dopant-free hole transporting materials for high-efficiency perovskite solar cells. Adv. Energy Mater. **8**, 1702512.
172. Zhang, J., Hu, X., Li, H., et al. (2021). High-performance ITO-free perovskite solar cells enabled by single-walled carbon nanotube films. Adv. Funct. Mater. **31**, 2104396.
173. Lin, Y., Bai, Y., Fang, Y., et al. (2018). Enhanced thermal stability in perovskite solar cells by assembling 2D/3D stacking structures. J. Phys. Chem. Lett. **9**, 654–658.
174. Zuo, L., Guo, H., deQuilettes, D.W., et al. (2017). Polymer-modified halide perovskite films for efficient and stable planar heterojunction solar cells. Sci. Adv. **3**, e1700106.
175. Wang, H., Rahaq, Y., and Kumar, V. (2016). A composite light-harvesting layer from photoactive polymer and halide perovskite for planar heterojunction solar cells. Sci. Rep. **6**, 29567.
176. Karani, A., Yang, L., Bai, S., et al. (2018). Perovskite/colloidal quantum dot tandem solar cells: theoretical modeling and monolithic structure. ACS Energy Lett. **3**, 869–874.
177. Jeng, J.-Y., Chiang, Y.-F., Lee, M.-H., et al. (2013). CH3NH3PbI3 perovskite/fullerene planar-heterojunction hybrid solar cells. Adv. Mater. **25**, 3727–3732.
178. Liu, C., Wang, K., Du, P., et al. (2015). Efficient solution-processed bulk heterojunction perovskite hybrid solar cells. Adv. Energy Mater. **5**, 1402024.
179. Wang, X.-D., Huang, Y.-H., Liao, J.-F., et al. (2019). In situ construction of a Cs_2SnI_6 perovskite nanocrystal/SnS_2 nanosheet heterojunction with boosted interfacial charge transfer. J. Am. Chem. Soc. **141**, 13434–13441.
180. Wu, S., Li, Z., Zhang, J., et al. (2021). Low-bandgap organic bulk-heterojunction enabled efficient and flexible perovskite solar cells. Adv. Mater. **33**, 2105539.
181. Liu, Y., Bag, M., Renna, L.A., et al. (2016). Understanding interface engineering for high-performance fullerene/perovskite planar heterojunction solar cells. Adv. Energy Mater. **6**, 1501606.
182. Yang, F., Yan, L., Zhang, B., et al. (2019). Fabrication of ternary $NaTaO_3$/g-C_3N_4/G heterojunction photocatalyst with enhanced activity for Rhodamine B degradation. J. Alloys Compd. **805**, 802–810.
183. Yuan, J., Zhang, X., Sun, J., et al. (2021). Hybrid perovskite quantum dot/non-fullerene molecule solar cells with efficiency over 15%. Adv. Funct. Mater. **31**, 2170196.
184. Wang, C., Xue, D., Shen, X., et al. (2019). White light-emitting devices based on ZnCdS/ZnS and perovskite nanocrystal heterojunction. Nanotechnology **30**, 465201.
185. Chen, W., Hao, J., Hu, W., et al. (2017). Enhanced stability and tunable photoluminescence in perovskite $CsPbX_3$/ZnS quantum dot heterostructure. Small **13**, 1604085.
186. Salazar-Rios, J.M., Sukharevska, N., Speirs, M.J., et al. (2018). Enhancing quantum dot solar cells stability with a semiconducting single-walled carbon nanotubes interlayer below the top anode. Adv. Mater. Interfac. **5**, 1801155.
187. Tan, Z.-K., Moghaddam, R.S., Lai, M.L., et al. (2014). Bright light-emitting diodes based on organometal halide perovskite. Nat. Nanotechnol. **9**, 687–692.
188. Kim, Y.-H., Cho, H., Heo, J.H., et al. (2015). Multicolored organic/inorganic hybrid perovskite light-emitting diodes. Adv. Mater. **27**, 1248–1254.
189. Song, J., Li, J., Li, X., et al. (2015). Quantum dot light-emitting diodes based on inorganic perovskite cesium lead halides ($CsPbX_3$). Adv. Mater. **27**, 7162–7167.
190. Wong, A.B., Lai, M., Eaton, S.W., et al. (2015). Growth and anion exchange conversion of $CH_3NH_3PbX_3$ nanorod arrays for light-emitting diodes. Nano Lett. **15**, 5519–5524.
191. Li, G., Rivarola, F.W.R., Davis, N.J.L.K., et al. (2016). Highly efficient perovskite nanocrystal light-emitting diodes enabled by a universal crosslinking method. Adv. Mater. **28**, 3528–3534.
192. Xiao, Z., Kerner, R.A., Zhao, L., et al. (2017). Efficient perovskite light-emitting diodes featuring nanometre-sized crystallites. Nat. Photonics **11**, 108–115.
193. Lin, K., Xing, J., Quan, L.N., et al. (2018). Perovskite light-emitting diodes with external quantum efficiency exceeding 20 per cent. Nature **562**, 245–248.
194. Luo, J., Wang, X., Li, S., et al. (2018). Efficient and stable emission of warm-white light from lead-free halide double perovskites. Nature **563**, 541–545.
195. Yao, E., Yang, Z., Meng, L., et al. (2017). High-brightness blue and white LEDs based on inorganic perovskite nanocrystals and their composites. Adv. Mater. **29**, 1606859.
196. Kim, H., Han, J.S., Choi, J., et al. (2018). Halide perovskites for applications beyond photovoltaics. Small Methods **2**, 1700310.
197. Wei, Y., Feng, G., Mao, P., et al. (2020). Lateral photodetectors based on double-cable polymer/two-dimensional perovskite heterojunction. ACS Appl. Mater. Interfaces **12**, 8826–8834.
198. Marunchenko, A.A., Baranov, M.A., Ushakova, E.V., et al. (2022). Single-walled carbon nanotube thin film for flexible and highly responsive perovskite photodetector. Adv. Funct. Mater. **32**, 2109834.
199. Jeon, I., Chiba, T., Delacou, C., et al. (2015). Single-walled carbon nanotube film as electrode in indium-free planar heterojunction perovskite solar cells: investigation of electron-blocking layers and dopants. Nano Lett. **15**, 6665–6671.
200. Acharyya, P., Kundu, K., and Biswas, K. (2020). 2D layered all-inorganic halide perovskites: recent trends in their structure, synthesis and properties. Nanoscale **12**, 21094–21117.
201. Luo, J., Zhang, W., Yang, H., et al. (2021). Halide perovskite composites for photocatalysis: a mini review. Ecomat **3**, e12079.
202. Wu, Y., Wang, P., Zhu, X., et al. (2018). Composite of $CH_3NH_3PbI_3$ with reduced graphene oxide as a highly efficient and stable visible-light photocatalyst for hydrogen evolution in aqueous HI solution. Adv. Mater. **30**, 1704342.
203. Xu, Y.F., Yang, M.Z., Chen, B.X., et al. (2017). A $CsPbBr_3$ perovskite quantum dot/graphene oxide composite for photocatalytic CO_2 reduction. J. Am. Chem. Soc. **139**, 5660–5663.
204. Hao, J., Kim, Y.-H., Habisreutinger, S.N., et al. (2021). Low-energy room-temperature optical switching in mixed-dimensionality nanoscale perovskite heterojunctions. Sci. Adv. **7**, eabf1959.

ACKNOWLEDGMENTS

This work was supported by the National Natural Science Foundation of China (NSFC, 62121005, 62134009, 61774155), and Natural Science Foundation of Jilin Province (20220101203JC).

AUTHOR CONTRIBUTIONS

W.Y. and T.W. conceived the project. W.Y. F.L., and T.H. wrote the manuscript. F.L., W.L., and T.W. revised the manuscript.

DECLARATION OF INTERESTS

The authors declare no competing interests.

LEAD CONTACT WEBSITES

https://people.ucas.edu.cn/~0064491 (W.Y.)
https://www.unsw.edu.au/staff/tom-wu (T.W.)